Review

# 1D and 2D Boron Nitride Nano Structures: A Critical Analysis for Emerging Applications in the Field of Nanocomposites

Gunchita Kaur Wadhwa, Dattatray J. Late,* Shrikant Charhate, and Shashi Bhushan Sankhyan

Read Online

ACCESS | Metrics & More | Article Recommendations

**ABSTRACT:** Boron nitride (BN) with its 1D and 2D nano derivatives have gained immense popularity in both the field of research and applications. These nano derivatives have proved to be one of the most promising fillers which can be incorporated in polymers to form nanocomposites with excellent properties. These materials have been around for 25 years whereas significant research has been done in this field for only the past decade. There are many interesting properties which are imparted to the nanocomposites wherein thermal stability, large energy band gap, resistance to oxidation, excellent thermal conductivity, chemical inertness, and exceptional mechanical properties are just a few worthy of mention. Hexagonal boron nitride (h-BN) was selected as the parent material by most researchers reviewed in this paper through which 2D derivative Boron nitride nanosheets (BNNS) and 1D derivative Boron nitride nanotubes (BNNTs) are synthesized. This review will focus on the in-depth properties of h-BN and further will concisely focus on BNNS and BNNTs for their various properties. A detailed discussion of the addition of BNNS and BNNTs into polymers to form nanocomposites, their synthesis, properties, and applications is followed by a summary determining the most suitable synthesizing processes and the materials, keeping in mind the current challenges.
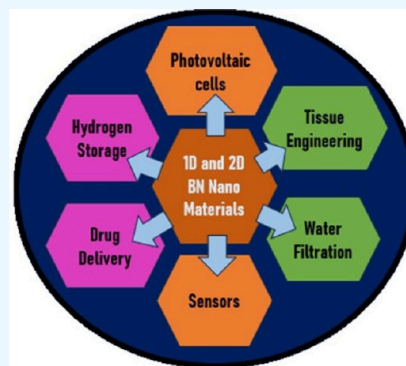
## 1. INTRODUCTION

Nanoscience is the modification of particles at the nano level wherein the properties of the material can be enhanced at macro level. These structures have proved to have extreme potential mechanically, electrically, optically, and thermally which can be further utilized in exceptional applications. Nanoscience, with its top-down approach, has gained immense popularity with its ability to achieve extensive variations in the properties of the materials.[1] Variations in terms of physical, electrical, and mechanical properties with varying particle size have led to immense applications in various fields such as the automotive, defense, aerospace, construction, and electronics industries, etc.[2−6] Another upcoming field in materials is polymers, in the form of composites, polymer matrix composites, nanocomposites, etc.[7] The dispersion of nano materials into the composites or forming a thin film on the polymer are a few methods which lead to materials with enhanced properties.[8,9]

Nano materials seem to be one of the most discussed fillers both in the field of research and in their applications in industry, especially BN. BN consists of an equal number of boron (B) and nitrogen (N) atoms and shares a similar structure with graphite. However, it differs in its bonding, as the N atomic nucleus and B atoms combine to form a strong sigma[10,11] bond through an $sp^2$ orbital. This bonding imparts a partially ionic character due to the electron pairs in $sp^2$ hybridized BN and weak van der Waals forces between

adjacent B and N atoms of different layers, giving rise to anisotropic properties. BN exists in four crystalline forms, namely hexagonal BN (h-BN), cubic BN (c-BN), rhombohedral BN (r-BN), and wurtzite BN (w-BN). The key distinction among these phases lies in their hybridization: h-BN and r-BN are dense phases with $sp^2$ hybridization, while c-BN and w-BN are low-density phases with $sp^3$ hybridized BN bonds.[12] Particularly intriguing is h-BN, as it shares a structural resemblance to graphite.[13] BN nanomaterials can be categorized into different dimensions: zero-dimensional (0D) such as nanospheres; one-dimensional (1D) like nanotubes, nanofibers, and nanoribbons; and two-dimensional (2D), including thin films and nanosheets. Figure 1 depicts the exfoliation of h-BN to form BNNTs and BNNS.[14] h-BN has proved to have excellent thermal stability and can withstand high temperatures without significant structural changes. It has a high decomposition temperature of around 900−1000 °C in an inert atmosphere. It is an excellent electrical insulator even at high temperatures and extreme conditions. In addition, h-
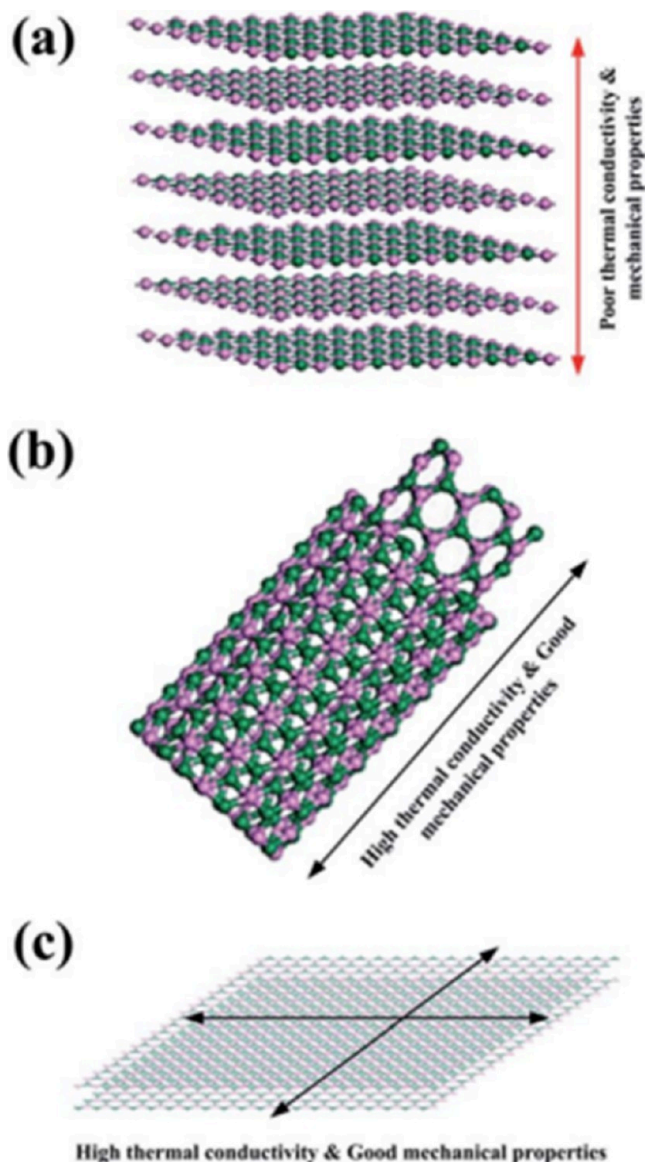
**Figure 1.** (a) High performance h-BN showing poor thermal conductivity and mechanical properties across vertical layers. (b) BNNTs with high thermal conductivity and good mechanical properties. (c) BNNS showing high thermal conductivity and good mechanical properties like BNNTs. Adapted/reprinted with permission from ref 29. Copyright (2014) Royal Society of Chemistry.

BN is transparent in the ultraviolet, visible, and infrared regions of the electromagnetic spectrum, making it useful for applications in optics and photonics. As a result, h-BN shows great promise as a scaffold for diverse functional materials with numerous potential applications. These applications encompass electronics[15,16], sensors[17,18], hydrogen storage[19,20], health-related technologies[21,22], as well as water and gas separation[23-28].

## 2. HEXAGONAL BORON NITRIDE

Boron nitride in its basic form is quite like graphite, with boron and nitride atoms placed alternatively replacing the carbon atoms.[30] This compound was prepared in 1840 with boric acid and potassium cyanide as base materials. Boron nitride due to its analogous behavior to graphite has become quite a popular research subject wherein B−N ionic bonding leads to a

comparable difference in the properties. Boron nitride is immiscible in water and exhibits tremendous chemical and thermal stability, high electrical resistivity, and thermal conductivity with a low dielectric constant.[11,31,32] Incorporation of BN to polymers has proven to improve its wear resistance. There are many nano derivatives that can be synthesized from the parent BN-like boron nitride ribbons, nanotubes, nano powder, and nanosheets. This paper will mainly focus on incorporation of boron nitride nanosheets (BNNS) and nanotubes (BNNT) to form transparent nanocomposites.

**2.1. Boron Nitride Nano Sheets (BNNS).** The two-dimensional nano derivative from h-BN is the BNNS as shown in Figure 2(a,b). These are analogous to graphene and can be
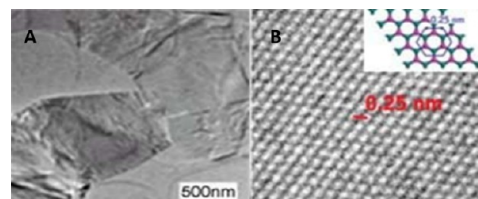


**Figure 2.** (a) BNNS sample under SEM with 500 nm magnification. (b) TEM image of BNNS keeping the electron beam perpendicular to the (002) plane, showing BNNS with a fringe separation of approx. 0.25 nm. Adapted/reprinted with permission fromref 34. Copyright (2009) Wiley.

produced in bulk via two main methods of preparation. BNNS can be prepared by either micro milling h-BN and sonicating with assisted exfoliation or by growing the same on or without a substrate via chemical vapor deposition method.[33] The main considerations while synthesizing BNNS is to monitor the size, shape, thickness, density, and alignment of the BNNS (Figure 3).

**2.2. Boron Nitride Nanotubes (BNNT).** Since the discovery of carbon nanotubes (CNTs), a constant stir was created to intensify the experimentation process on similar structures.[36-38] The major concern depicted with CNTs was the variation in electrical properties with a slight variation in the chirality or tube diameter. As a wide-range of properties could be achieved due to this feature, the implementation of CNTs for various applications became intricate as the diameter and the chirality of the tubes were difficult to monitor. This led to the development of BNNT. Their structure is like that of graphite wherein B and N replace the carbon atoms forming an sp$^2$ trigonal planar structure.[39] Their first discovery was with an inner diameter of 1−3 nm (Figure 4) and length up to 200 nm with an energy gap of 5.5 eV.[40] BNNTs exhibit similar structures as CNTs with their properties independent of the diameter of the tube (Figure 5), their chirality, the number of tubes, and the resistance to oxidation at elevated temperatures. This suggests the implementation of BNNTs for various applications wherein thermal and chemical stability are basic criteria, such as in nanocomposites, NEMS, biomedical uses, and many more.[40-44]

**2.3. Synthesis of BNNTs.** One of the first methods through which BNNTs were synthesized is the arc discharge method wherein BNNTs were grown through using cooled copper and BN packed tungsten as electrodes.[46] Many successful attempts were made after this wherein some modified the above method like the modified arc discharge method[47-50] and the rest were different, such as autoclav-
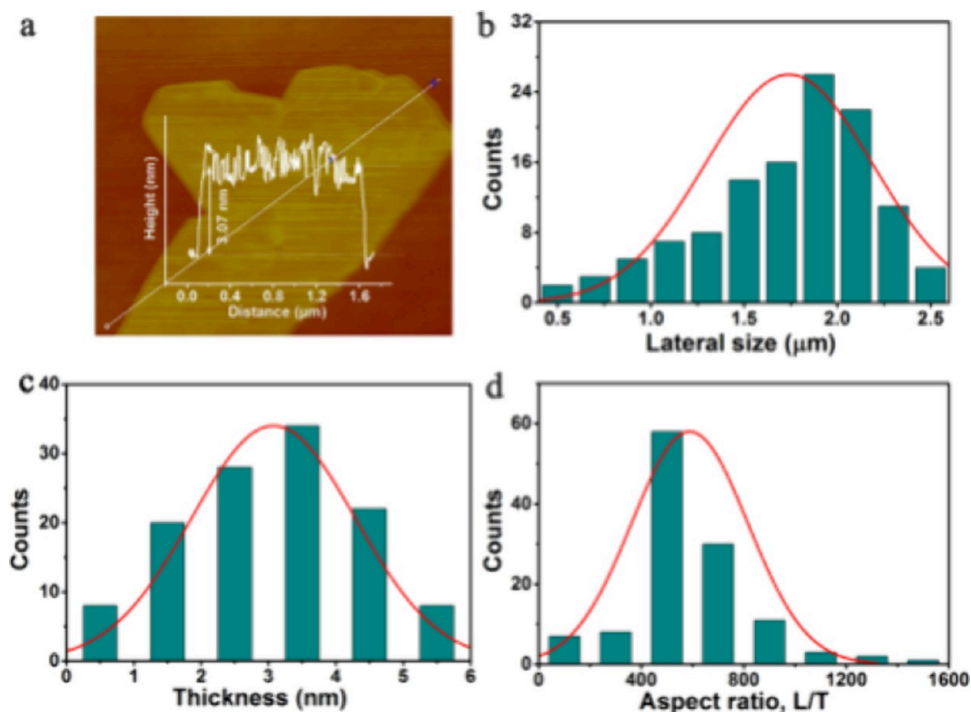
**Figure 3.** (a) AFM images of BNNS, (b) histograms of measured values for nanosheets length, (c) histograms of measured values for nanosheets thickness, and (d) aspect ratio (length/thickness). Adapted/reprinted with permission from ref 35. Copyright (2018) Nature.
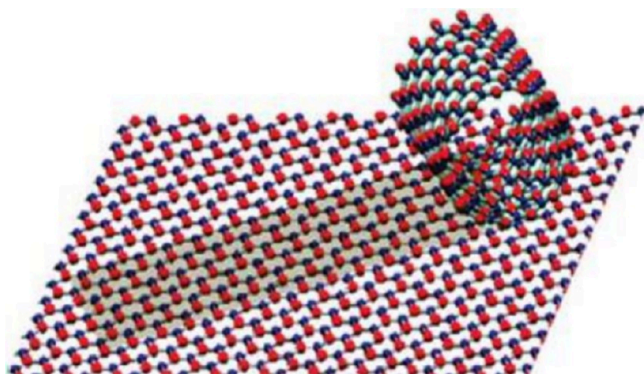


**Figure 4.** BNNT with alternating boron and nitrogen atom rolled hexagonal lattice. Adapted/reprinted with permission from ref 30. Copyright (2010) American chemical society.

ing[51−53], template synthesis,[54−56] plasma jet method,[57,58] laser ablation[59−63] ball milling,[64−67] chemical vapor deposition,[68−72] etc. Some of the methods through which controlled synthesis and mass production of BNNTs are achieved are discussed as follows.

*2.3.1. Thermal Annealing and Chemical Vapor Deposition.* One of the most successful methods is the boron oxide-assisted chemical vapor deposition (BOCVD)[73,74] as it was able to produce BNNTs in gram yields. A vertical induction furnace is used in this process where a BN crucible is placed in the bottom with boron and magnesium oxide loaded in the crucible. This is heated to 1300 °C forming boron oxide and magnesium vapors which are further reacted with ammonia in an argon-controlled chamber at low temperatures. This separates boron from boron oxide and promotes the growth of highly pure BNNTs. This method was further enhanced by Zhi et al.[75] to produce BNNTs with further reduced impurities[76] producing grams of it at the laboratory level.[77]



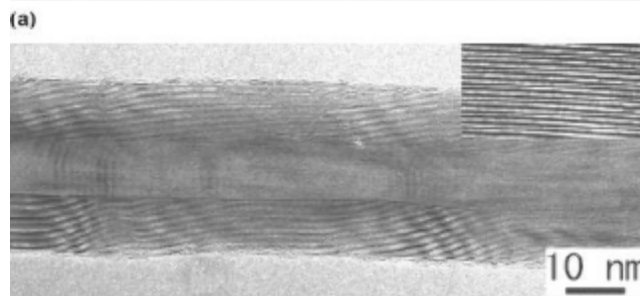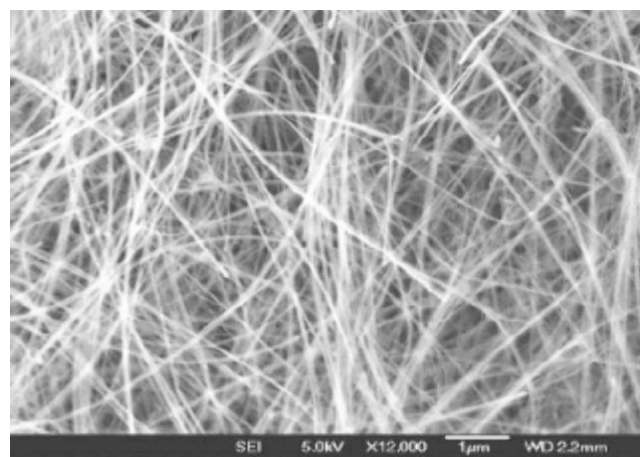**Figure 5.** (a) The typical scanning electron microscope (SEM) image of BNNTs synthesized by BOCVD (bottom-up chemical vapor deposition) method. (b) The high-resolution transmission electron microscope (TEM) image of BNNTs synthesized by BOCVD method. The inset shows an enlarged portion of a BN tubular wall, providing a closer view of the nanotube structure. Adapted/reprinted with permission from ref 45. Copyright (2006) Springer.

Nevertheless, the commercialization and practical application of BNNTs in the industry face obstacles due to their comparatively lower production rate and the requirement for specialized chamber designs (Figure 6).
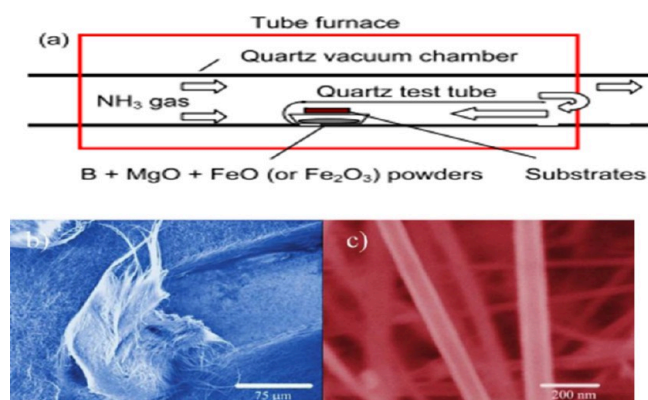


**Figure 6.** (a) The experimental setup used for BNNT growth in a horizontal tube furnace. Adapted from ref 78. (b) SEM image showcasing the tubular structure of BNNTs with amorphous free side walls. (c) SEM image of hollow dense BNNT structure. Adapted/reprinted with permission from ref 79. Copyright (2010) ACS Publication.

Lee et al. presented a successful method for producing high-purity BNNTs using a conventional resistive tube furnace at 1200 °C.[78] The key aspect of this technique is the application of catalytic chemical vapor deposition (CCVD), where a closed-end quartz test tube is utilized to trap and confine the growth vapors, facilitating the formation of BNNTs. This approach is referred to as the growth vapor trapping (GVT) approach. By incorporating catalytic nanoparticles (MgO, Fe, Ni) coated on Si substrates, the GVT growth of BNNTs can be precisely controlled through the vapor−liquid−solid (VLS) process. This controlled approach differs significantly from the original BOCVD method, where BNNTs are formed through spontaneous nucleation/condensation. Furthermore, they achieved a breakthrough by demonstrating patterned growth of BNNTs on a Si substrate using CVD for the first time.[79] The CCVD/GVT method is highly effective in producing BNNTs with exceptional quality and purity at specific, predetermined locations. Moreover, the GVT approach offers the advantage of easy reproducibility in various research laboratories, as the setup is relatively simple and straightforward.[81] The BNNT films display superhydrophobic characteristics attributed to two main factors. First, their nanoscopic surface roughness, as depicted in Figure 7, contributes to the creation of a water-repellent surface.[82] Additionally, the films exhibit reduced surface energy caused by the formation of adsorbates, further enhancing their superhydrophobic properties.[80]

Another approach for the synthesis of BNNTs, first introduced by Chen et al. in 1999 involves the high-temperature ball milling process.[83] Over time, this method has been further developed and refined by incorporating boron ink.[84−87] The process entails ball milling boron powder under an $N_2/NH_3$ atmosphere for an extended duration, which can be up to 150 h. Subsequently, the milled boron powder is mixed with ferric nitrate (Fe $(NO_3)_3$) and cobalt nitrate (Co $(NO_3)_2$) in ethanol to create B ink. The B ink is then subjected to treatment with $N_2/NH_3$ at temperatures ranging from 1000
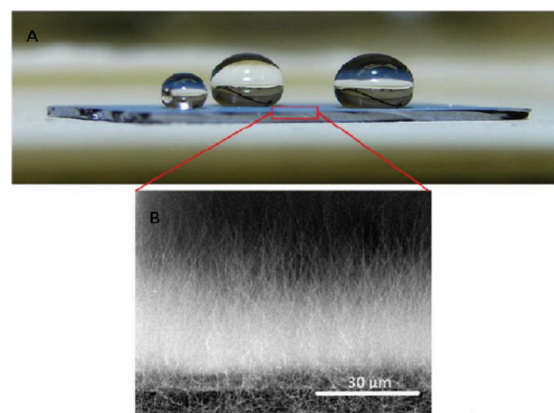


**Figure 7.** (a) A photograph demonstrating the superhydrophobic nature of a BNNT film produced by CCVD. (b) A zoom-in cross-sectional view of BNNTs grown on a silicon substrate, revealing the vertical alignment of the BNNTs on the substrate surface. Adapted/reprinted with permission from ref 80. Copyright (2012) ACS Publication.

°C to 1300 °C for several hours to facilitate the conversion into BNNTs. Additionally, B ink can be applied onto various surfaces to deposit BNNTs.[86]

*2.3.2. Laser Vaporization with Pressurized Vapor/Condenser Method.* Since 1996, the laser ablation or laser evaporation technique has been employed for the growth of BNNTs, drawing inspiration from the growth process of carbon nanotubes (CNTs) followed by the work of many researchers.[88−91] In 2005, Yap et al. achieved a significant breakthrough by demonstrating the first successful patterned growth of BNNTs on substrates using iron catalysts and pulsed-laser deposition of a BN target.[92] This catalytic pulsed-laser deposition (PLD) approach enabled the formation of fine BNNTs with diameters ranging from ∼10 to 20 nm, at relatively low substrate temperatures of about 600 °C.

In 2007, Arenal et al. reported a root-based growth mechanism for single-wall BNNTs through laser heating under $N_2$ at 1 atm.[88] A notable advancement in the synthesis of BNNTs was achieved in 2009 through a modified laser evaporation technique.[93] This method, later referred to as the high temperature/high pressure (HTP) method, utilized the pressurized vapor/condenser (PVC) approach. In this process, a high-powered laser, either a 1 kW free-electron laser with a wavelength of 1.6 $\mu$m or a kW-class $CO_2$ laser with a wavelength of 10.6 $\mu$m, was used to vaporize a boron (or BN) target within a chamber filled with high-pressure nitrogen (pressure ranging from 2 to 20 bar). The intense laser vaporization resulted in the production of a hot boron vapor stream at temperatures of approximately 4000 °C, which then condensed into liquid boron droplets, serving as nucleation sites. These boron droplets, aided by the elevated nitrogen pressure, rise upward and rapidly form BNNTs. To promote the growth of BNNT fibrils, a cooled metal wire is introduced through the boron plume in the chamber, acting as a condenser. The condenser can be made from various materials such as BN, B, stainless steel, copper niobium (Cu−Nb), and tungsten (W), in different shapes like wires, sheets, ribbons, and rods. The production rate typically ranges from 20 to 120 mg/h. The resulting BNNTs appear as tube bundles and an entangled network of fibrils (Figure 8).
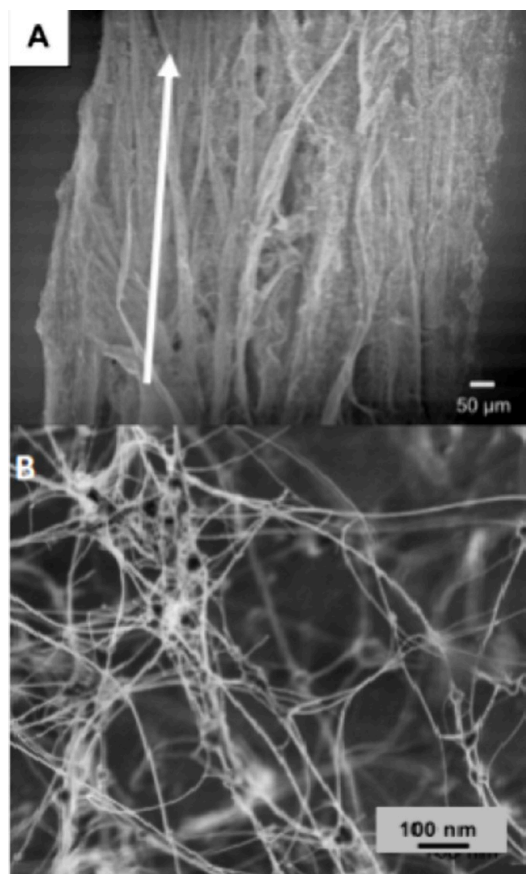
**Figure 8.** (a) SEM image of BNNT fibrils produced by the pressurized vapor/condenser method (PVC). The white arrow indicates the growth direction, which is parallel to the BNNT fibrils. (b) SEM image of the entangled network of BNNTs also produced using the pressurized vapor/condenser method (PVC). The short arrow highlights a round, solidified boron droplet presents within the network. Adapted/reprinted with permission from ref 94. Copyright (2009) IOP Science.

Recently, the PVC/HTP method has undergone further modifications, introducing a new high-pressure chamber with a pressure of 1000 psi or 68 atm. This upgraded setup utilizes a 2.5 kW diffusion-cooled $CO_2$ slab laser as the energy source.[95]

*2.3.3. Large Scale Synthesis by Inductive Thermal Plasma Method.* The torch method was utilized for large-scale synthesis of small-diameter BNNTs, measuring approximately 5 nm, at an impressive rate of 20 g/h. The process involved feeding solid hexagonal boron nitride (h-BN) powder, along with $N_2$ and $H_2$ gases, into a high-temperature induction plasma with temperatures exceeding 8000 K and operating at

atmospheric pressure.[96] The high-temperature plasma decomposed all the precursor materials into their constituent elements (B, N, and H), leading to the condensation of nanosized boron droplets downstream of the reactor, where the temperature gradient was notably large at 105 K/s. These boron droplets served as nucleation sites for the formation of BNNTs.

It was claimed that hydrogen gas played a crucial role in this process by acting as a catalyst. It formed an intermediate H—B—N species, which hindered the recombination of N radicals generated from the $N_2$ feedstock or from the dissociation of h-BN.

A similar technique using inductively coupled plasma for BNNT synthesis was independently reported in 2014.[97] In this method, a customized extended pressure inductively coupled plasma (EPIC) system was constructed, capable of producing plasma with power ranging from 40 to 50 kW. By flowing $N_2$ gas at a rate of 50 L per minute, a $N_2$ plasma plume was generated. Boron feedstock, such as amorphous boron or h-BN powder, was injected into the plasma plume at rates ranging from 100 mg/min to 1700 mg/min, using $N_2$ as the carrier gas at pressures varying from 14.7 to 75 psi absolute. Under high $N_2$ pressure, molten boron droplets formed within the plasma plume, which reacted with $N_2$ to create BNNTs, resulting in a remarkable growth rate of 35 g per hour.[97]

**2.4. Synthesis of BNNS.** Borazine was used to grow one ever BNNS kind of structure on a metal substrate.[98] The two most prominent methods, mechanical and chemical exfoliation, are used to form BNNS.[99] The former utilized a Scotch tape to peel the layers of the BN sample[100−102] or exfoliate BN and further ultrasonicate to achieve BNNS layers,[34,103] whereas the latter utilizes molten hydroxides for the same.[104] This review will briefly discuss the methods of synthesizing BNNS.

1. Mechanical Exfoliation: This method involves direct by applying forces in the material causing mechanical exfoliation[105−107] and other exfoliation techniques use shear forces which reduce the size.[86,108] Ball milling is a highly effective approach for exfoliating bulk h-BN material into few-layered sheets. Urea is found to be one of the most popular mixtures of h-BN as the smaller molecules of urea can easily penetrate the interlayer defects of h-BN assisting efficient exfoliation.[109,110]

It is noteworthy (Figure 9) that the thickness of BNNS has a direct relation with the properties whereas the thickness of the BNNS is defined by the method of synthesizing and further the time duration for which processes like ball milling are performed of the BNNS is defined by the method of synthesizing and further the time duration for which processes like ball milling are performed, low-energy ball milling and integration with sonication have been used to obtain high-yield
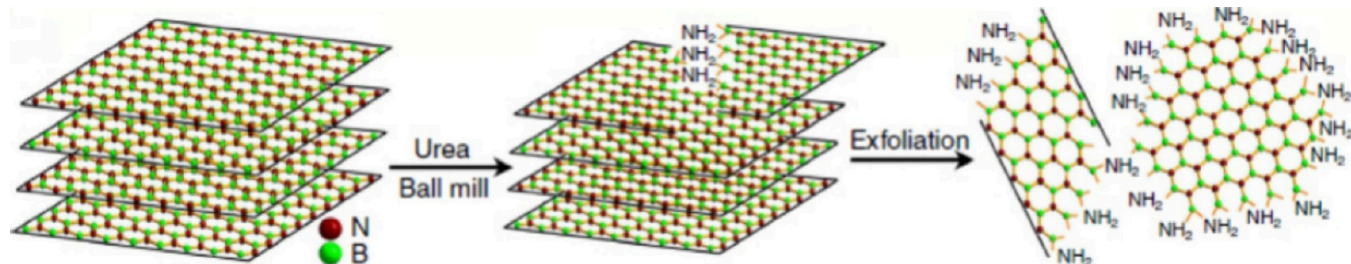


**Figure 9.** Urea assisted ball milling. Adapted/reprinted with permission from ref 99. Copyright (2022) Chemistry Europe.
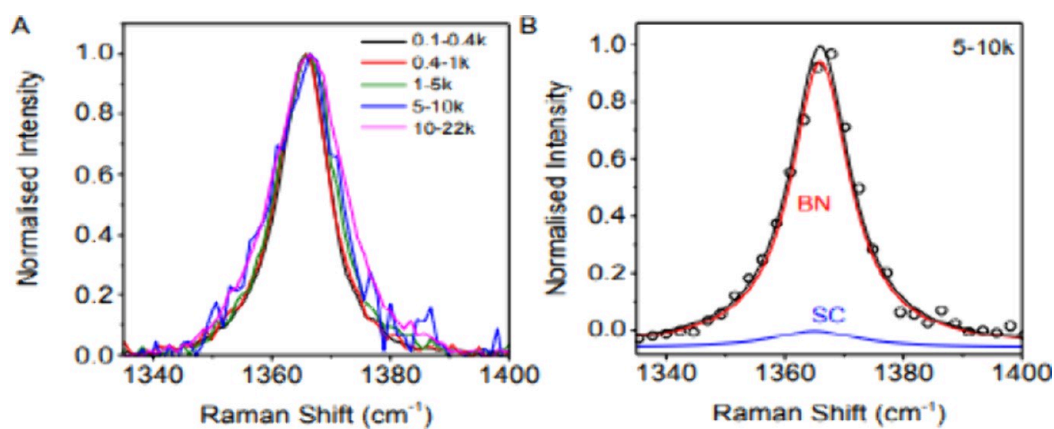
**Figure 10.** (a) Results of Raman Spectroscopy based ranging for different sizes and (b) results of Raman spectroscopy for BNNS dispersed normal to the maxima peak at G Band Frequency. Adapted/reprinted with permission from ref 111. Copyright (2018) ACS Publication.
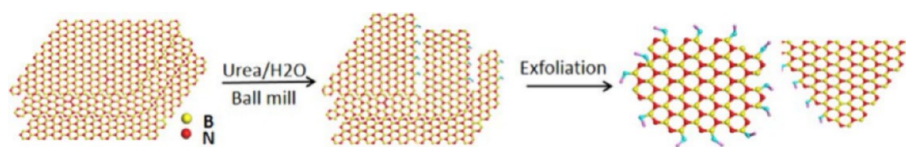


**Figure 11.** Schematic representation of BNNS from h-BN via ball milling. Adapted/reprinted with permission from ref 117. Copyright (2019) IOP Science.
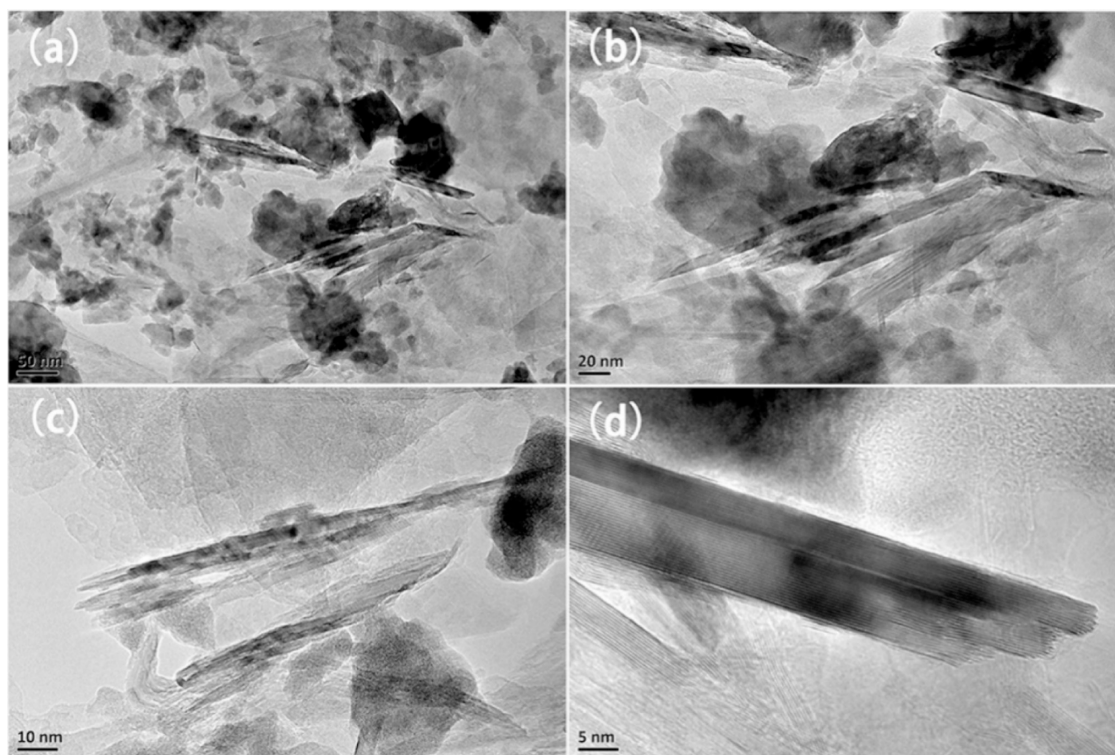


**Figure 12.** TEM images of ball milled commercial h-BN sample to BNNS under (a) 5000× magnification, (b) 12 500× magnification, (c) 25 000× magnification, and (d) 50 000× magnification. Adapted/reprinted with permission from ref 118. Copyright (2021) ACS Publications.

and high-quality BNNS[87] (Figure 10). The BNNS achieved after the process of ball milling wherein organic dispersion solvents are used can lead to successful exfoliation of h-BN, but the milling is not homogeneous and isotropic in a particular direction.[99] In some cases, the XRD results done on the ball milled sample show an increase in the width of the peak suggesting the presence of defects and many petite samples of

BNNS which is also confirmed with the help of SEM and TEM[109] (Figure 11). Recently BNNS exfoliated via utilizing thionyl chloride as the liquid medium have found their way into applications wherein large lateral dimensions of BNNS are needed.[112−114] These BNNS obtained are not suitable for nanocomposite films fillers wherein high thermal transport is the prime criteria.[110,115,116] The above research supports the

effectiveness of the method of ball milling as the mechanical forces break more inter layer bonds due to weak Vander walls forces than intra layer bonds. To further improve the quality of BNNS obtained from this process by regulating the mechanical forces applied and by selecting appropriate dispersing agents resulting in high aspect ratios and better lateral dimensions.[99] Figure 12 highlights the TEM imaging of the ball milled BNNS sample.

2. Liquid Exfoliation: BNNS can be successfully obtained using different solvents. Many researchers have experimented with the same to produce the results wherein solvents such as 1,2-dichloroethane,[119] water,[120] sodium dodecyl sulfate (SDS)−water solutions,[121] N,N′-dimethylformamide (DMF)[34], sulfonic acid, and methanesulfonic acid[122] have been used to exfoliate h-BN to BNNS. The selection of solvents is essential for effective exfoliation which forms the basic criteria for the output of BNNS obtained and the Hansen solubility parameter (HSP)[123] theory is used to understand their functions in h-BN exfoliation. Liquid exfoliation uses effective exfoliation agents like isopropyl alcohol (IPA). IPA is one of the most effective solvents. The surface energy of IPA is very similar to that of nanosheets which in turn reduces the van der Walls forces of attraction between
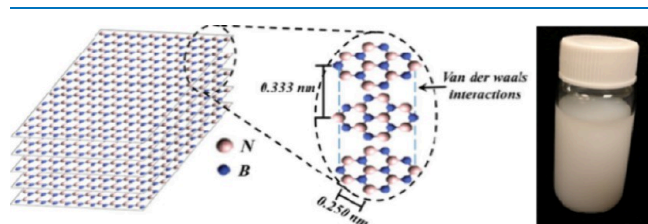


**Figure 13.** Crystal Structure representation of h-BN on the left. Aqueous solution of BNNs obtained from sonication of h-BN in IPA on the right. Adapted/reprinted with permission from ref 99. Copyright (2022) Chemistry Europe.

the interlayered sheets of boron nitrite thereby reducing the energy required for exfoliation (Figure 13).[99,124,125]

Furthermore, epitaxial growth of monolayer h-BN has been demonstrated on preferred substrates like Pt,[111,126] Ru (001), and Ni[111,127] using borazine as the precursor. Many of the solvents are excluded due to their high cost, toxicity, and high boiling point. One of the important conclusions derived was that the surfactants play a major role in the stabilization of the aqueous solution and a minor role in the process of exfoliation.[99] Many have discussed the use of polymers like polybutadiene, poly(styrene-co-butadiene), poly(vinyl chloride), poly(vinyl acetate), PMMA, etc. in water or organic solvents for the process of exfoliation. The results for the same have been found up to the mark wherein many hurdles were observed. The main is the extraction of these added polymers from the exfoliated samples.[128−131] Out of all the above stated exfoliations, isopropanol (IPA) is found to have the maximum efficiency out of all the solvents.[99]

3. Chemical Vapor Deposition (CVD): Growing a single layer of Epitaxial h-BN can be achieved on substrates like Pt,[111] Ru (001), and Ni[111] by adsorption and decomposition of borazine.[132] Traditionally, Cu and Ni foils are one of the most popular choice of substrate for

the growth of two-dimensional hexagonal boron nitride (h-BN) due to their cost-effectiveness and excellent catalytic properties.[133,134] Further experimentation have led to identification of many substrates, including Pt[135,136] Ni and Cu.[137,138] Wang et al.[92] achieved the preparation of a triangular monolayer single crystal h-BN measuring 20 mm by thermal annealing Cu foils, and the size of the h-BN varied depending on the annealing time.

**2.5. Properties of BNNS and BNNT.** Boron nitride therefore due to its analogous behavior as graphite has become a quite popular research subject wherein B−N ionic bonding leads to a comparable difference in various properties of the two materials.

*2.5.1. Electrical Properties of BNNTs and BNNS.* One of the most discussed properties of boron nitride materials is the wide band gap which further induces an internal electrical insulation in the material.[139−142] Polarization effects of BNNTs (Figure 6) have proven to drastically increase the adhesion between the nano tubes and the matrix polymer which show much more promising results than CNTs.[143] This adhesion has further increased the interfacial bond between the nano tubes and the matrix polymer forming a composite with higher mechanical strength than that with CNTs.

The defects and the edge effects of the matrix polymer make BNNS the most superior 2D dielectric material.[144,145] A similar internal electrical insulation is observed in BNNS as well, which continues to perform the best until excessive defects or excessive edge effects hamper the same.

Therefore, both of the filler derivations of BN can be preferred in polymer composites to enhance dielectric properties.

*2.5.2. Thermal Properties of BNNTs and BNNS.* Both of the nano derivatives of the BN structure show excellent resistance to oxidation at higher temperatures with exceptional structural stability. BNNTs can withstand a temperature of 800 °C and monolayer BNNS can withstand temperatures up to 850 °C in air.[146−148] BNNTs and BNNS therefore are two of the most preferred fillers wherein high-performance oxidation resistant coatings are required.[149]

A direct relation was observed between the increase in the oxidation at slightly lower temperatures when the number of layers of BNNS are increased.[150] A drastic decrease in BNNTs decomposition temperature can be observed at 1000 °C to 1700 °C when placed in a sturdy electric field as it hampers the partial ionic bonds.[151]

A major difference between the predicted thermal conductivity and the actual experimental thermal conductivity is observed. The thermal conductivity of BNNTs was predicted to be 6000 $WmK^{-1}$[152−154] wherein the experimental results[155−157] proved the results to be around 200 $WmK^{-1}$ for MWBNNT with a 40 nm diameter.

A direct relation between the diameter of the BNNTs and thermal conductivity is observed where reduced diameter will have higher is the thermal conductivity therefore single walled nano tubes have higher thermal conductivity than multiwalled nanotubes and CNTs (Figure 14). An interfacial thermal resistance drastically reduces the thermal conductivity if BNNTs are used collectively.[158,159]

BNNS have demonstrated a varied range of thermal conductivities in various experiments with no concrete results.[160,161] One of the key factors observed to play a role in the determination of a relatively lower thermal conductivity
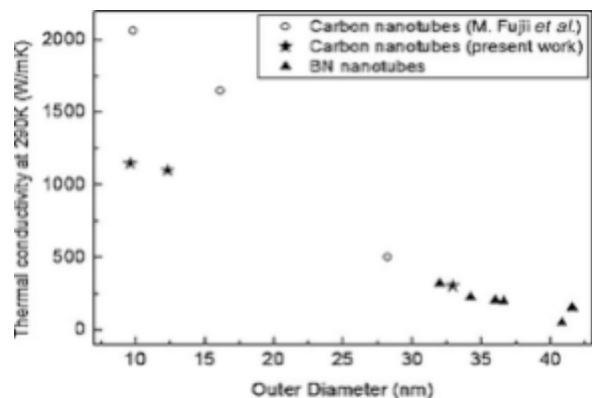
**Figure 14.** Graph displaying the thermal conductivity of BNNTs (boron nitride nanotubes) at 290 K (Kelvin) in comparison to their outer diameter. Adapted/reprinted with permission from ref 156. Copyright (2006) *Phys. Rev. J.*

than their carbon counterpart is molecular dynamics. A strong phonon scattering restriction is observed between the layers of BNNS which can be improvised by isotopic enrichment.[162,163]

Even with ambiguous results single layered BNNTs and BNNS improve the thermal conductivity when used as fillers in polymers for thermally conductive and electrically insulating composites.

*2.5.3. Mechanical Properties of BNNTs and BNNS.* BNNTs and BNNS both seem to exhibit excellent mechanical properties in terms of Young's modulus. Theoretical values of 0.837–0.912 are reported[164−168] further due to larger scattering BNNTs seem to perform better in extreme deformation conditions and at high temperatures. A range of data in terms of Young's modulus is observed which seems to vary with the method of synthesis adopted. A similar result is seen in the case of BNNS wherein the method adopted for synthesis varied the bending modulus.[169−171] The mechanical properties in the case of BNNS seem to also depend on the sheet thickness wherein the increase in the thickness of the sheet size decreases the bending modulus. This is due to the stacking defects within the layers of BNNS. Therefore, thin BNNTs and BNNS are preferred when a reinforcement option is to be considered in polymers for optimum mechanical results.

*2.5.4. Optical Properties of BNNTs and BNNS.* The constant energy band gap with less impurities imparts the white color to both these Nano derivatives of BN.[172] Both of these show photoluminescence and cathodoluminescence under UV light.[173−177] The method of synthesis is responsible for the optical properties wherein the wavelength emitted depends on the method of synthesis. With increasingly thinner the BNNS sheets, better investigation of the quantum properties can be made.

UV radiation is one of the emissions received on the earth's surface via the Sun. The spectrum of UV radiation is further subdivided into the three categories of UVA (315−400 nm), UVB (280−315 nm), and UVC (100−280 nm). Out of which UVB is largely blocked by glass but more than 50% of UVA can penetrate through glass. These radiations are classified according to their wavelength wherein the shorter the wavelength, the more harmful they become. There are many factors that determine the impact of UV radiation such as time of the year and of the day, latitude, altitude, clouds, and haze etc.[179]

Incorporation of both BNNS and BNNTs in composites or as thin films can lead to transparent polymers which can be used to shield for UV blocking (Figure 15). Channelizing the property of the BNNS by coating the polymers will be the focus of this paper.
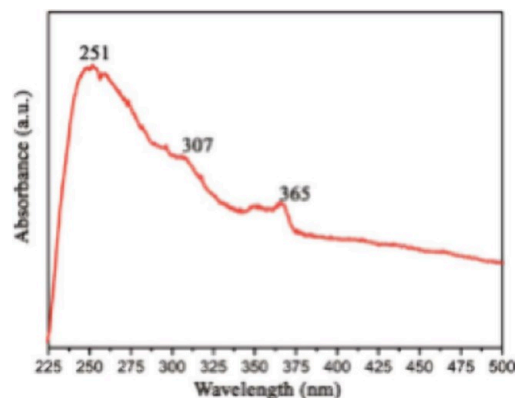


**Figure 15.** UV spectroscopy of BNNS. Adapted/reprinted with permission from ref 178. Copyright (2018) IOP Science.

## 3. NANOCOMPOSITES AND THEIR SYNTHESIS METHODS

Nanocomposites are composite materials in which at least one of the constituents has nanometric dimensions. The matrix is generally the base, and the strength is provided nanometrically. Nanofillers are added to improve various physical properties like the mechanical, thermal, and physicochemical properties of the resulting materials.[180−184] The process of nano-composite synthesis involves ensuring the uniform distribution of nanofillers within a polymer or ceramic matrix. Nano-composites are categorized based on the types of nanofillers and matrix materials employed. Specifically, two main classes of BN nanocomposites are discussed here, determined by the chosen matrix material: polymer-based and ceramic-based nanocomposites. This paper focuses on polymer based nano composites.

**3.1. Polymer Based Nanocomposites.** Polymer-based nanocomposites consist of a polymer matrix that acts as a base for the material and nanofillers, such as BN nanomaterials, as reinforcements. Polymers possess appealing properties like being lightweight, ease of processing, corrosion resistance, ductility, and cost-effectiveness. Additionally, they exhibit gas barrier properties, heat resistance, and fire resistance.[185,186] However, their main drawback lies in their low thermal and electrical conductivities.[187] By incorporating nanofillers as reinforcing agents into a polymer matrix, the resulting nanocomposite's properties are significantly enhanced. As mentioned previously, nanofillers can be categorized into three classes based on their dimensionality: 0D (spherical particles), 1D (nanotubes and fibers), and 2D (nanosheets). The selection of the reinforcement material depends on the intended application. When reinforcing a polymer matrix, several crucial factors come into play:

  (i) The properties of the polymer itself.
  (ii) The characteristics and the percentage by weight of the nanofiller added reinforcement.
 (iii) The average particle size, orientation, and distribution of the nanofillers added to the polymer matrix.[188]
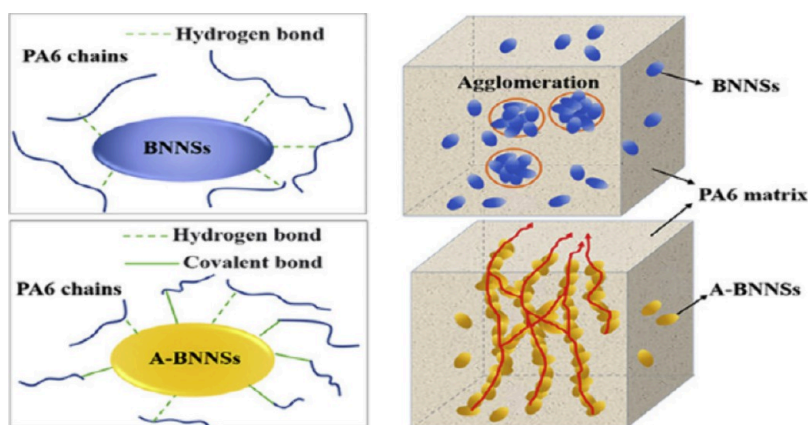
**Figure 16.** Nanocomposites depicted in the image are composed of nylon-6 (PA6) along with hexagonal boron nitride nanosheets (h-BNNS) or amino-functionalized h-BNNS (A-BNNS). Adapted/reprinted with permission from ref 190. Copyright (2018) ACS Publications.
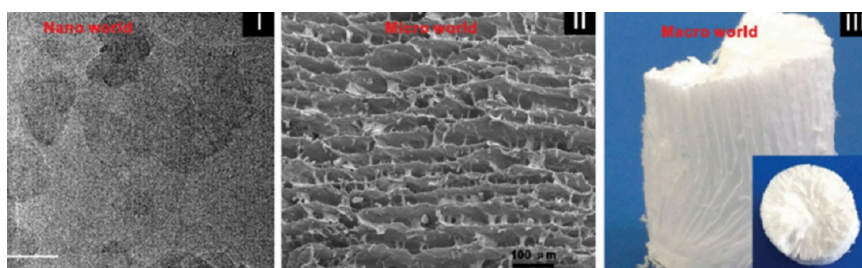


**Figure 17.** Hierarchical structures of the free-standing 3D-BNNS aerogel are depicted as follows: (I) Transmission electron microscopy (TEM) image of the BNNS. (II) Scanning electron microscopy (SEM) image of the 3D-BNNS aerogel, captured from a direction perpendicular to the ice growth. (III) Photograph of the 3D-BNNS aerogel. Adapted/reprinted with permission from ref 192. Copyright (2015) Wiley.

## 3.2. Synthesis of Polymer Based Nanocomposites.

Polymer Nanocomposites are manufactured using various methods, which can be broadly categorized into four main routes: melt intercalation/blending, in situ polymerization intercalation, template synthesis, and solvent mixing. Additionally, more recently, sonication and high-shear mixing have been suggested as alternative techniques to produce (bio)-nanocomposite materials. In this review, the emphasis will be on the techniques employed to create polymer-based nanocomposites utilizing BNNTs and BNNS as nanofillers to improve their properties.

### 3.2.1. Melt Intercalation/Blending.

Melt intercalation stands out as the most widely utilized method for synthesizing thermoplastic polymer-based nanocomposites. This approach typically involves three main steps: first, annealing the polymer matrix at high temperatures, followed by the addition of nanofillers, and finally, blending the composite to achieve a uniform distribution.[189] For example, h-BN can be integrated into a polymer matrix through the preparation of thermoplastic polyurethane (TPU) nanocomposites containing nano-h-BN. This is accomplished by melt blending using a corotating twin-screw extruder, and then forming thin TPU/h-BN films via hot pressing techniques.

In their study, Wang et al.[190] enhanced the thermal conductivity and mechanical properties of nylon-6 (PA6) through a two-step process (Figure 16). They first performed surface functionalization of BN nanosheets (BNNS) with amino groups, followed by melt blending with PA6. As a result of the amino functionalization, the BN nanosheets were better dispersed in the polymer matrix compared to nonfunctionalized BNNS as shown. This significant improvement in

dispersion led to a nearly 10-fold increase in thermal conductivity and thermal stability of the PA6/A-BNNS nanocomposites.

### 3.2.2. In-Situ Polymerization.

This technique allows efficient dispersion of nanofillers within the polymer matrix. Typically, nanomaterials are combined with a neat monomer or a monomer solution, and the mixture is then polymerized using heat, radiation, or an organic initiator. This method offers several advantages for preparing BN/polymer-based nanocomposites, especially the formation of strong interactions between BN nanoparticles and the polymer matrix through covalent bonds. Additionally, it helps to suppress particle aggregation by enabling the controlled growth of polymer chains around the nanoparticles. However, further research is required to address the solvent removal process in this method.[10]

### 3.2.3. Template Synthesis.

Templating is a technique used in the production of nanostructured materials. It utilizes a pre-existing pattern or template as a guide to shape the nanomaterials for the synthesis process. This method imparts precise control over the size, shape, and arrangement of nanomaterials, resulting in well-defined and tailored nanostructures with enhanced properties for various applications. The method of templating is commonly used to synthesize nanomaterials with well-defined size, shape, and configuration. This process involves three main steps: (i) creating building blocks, (ii) assembling building blocks guided by templates, and (iii) removing the template if necessary.[191]

Zeng et al. described a method for developing 3D-BNNS networks using an ice-templated approach. First, anisotropic freezing was done by using liquid nitrogen as a cryogen and
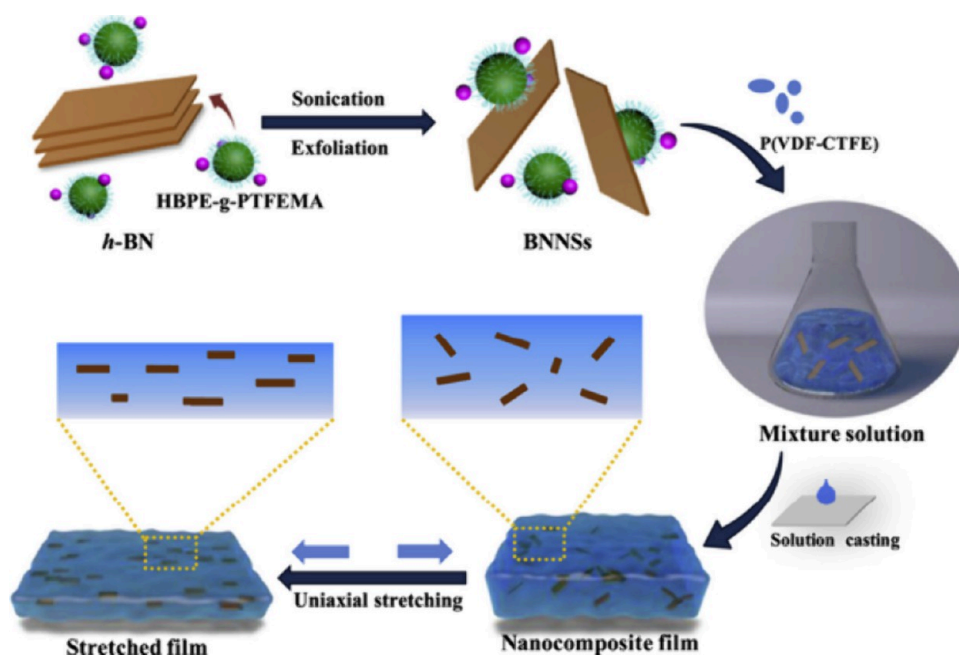
**Figure 18.** Process involves exfoliating BNNS in dimethylformamide (DMF) using a fluoro-hyperbranched polyethylene-*graft*-poly(trifluoroethyl methacrylate) (HBPE-*g*-PTFEMA) as a stabilizing agent. Preparation of Stretched BNNS/P(VDF-CTFE) Nanocomposite Film: This process entails creating a nanocomposite film composed of BNNS embedded in a poly(vinylidene fluoride-chlorotrifluoroethylene) (P(VDF-CTFE)) polymer matrix. To achieve the desired orientation of BNNS within the film, the material is uniaxially stretched at a constant temperature, allowing for controlled alignment of the nanosheets along the direction of deformation. Adapted/reprinted with permission from ref 197. Copyright (2020) IOP Science.

pouring a nonfunctionalized BNNS (NF-BNNS) aqueous slurry into a Teflon mold. During the freezing process, the suspended NF-BNNS and poly(vinyl alcohol) (PVA) were expelled from the growing ice crystals, allowing for precise directional ice growth (Figure 17). The frozen samples were then freeze-dried to obtain the BNNS aerogel scaffolds. These aerogel scaffolds were then sintered to form 3D-BNNS aerogels, which were subsequently immersed in an epoxy solution matrix. The resin infiltrated the aerogel scaffold, resulting in the formation of 3D-BNNS aerogel nanocomposites.[192]

The emulsion templating approach for producing nanocomposites is particularly intriguing due to several advantages it offers. One significant benefit is that this method circumvents the need for multiple sintering steps, streamlining the fabrication process. Additionally, it eliminates the use of harmful solvents, making it a more environmentally friendly and safer approach.[193]

*3.2.4. Solvent Mixing.* The solvent mixing method is an effective technique for dispersing nanofillers, especially layered materials, into polymer matrix nanocomposites. Nanofillers, often in a layered structure, are exfoliated by intercalating an organic compound into their interlayer spaces. This process results in the dispersion of well-separated plate-like particles. The exfoliated material is then dispersed in a solvent and mixed with a polymer solution. The polymer chains intercalate into and displace the solvent within the layered material. After removing the solvent, a multilayered structure is obtained, with the polymer chains trapped within the exfoliated material. The resulting nanocomposites exhibit reinforcement due to the large contact surface area between the polymer matrix and the exfoliated material.[10]

Using the polymer intercalation approach, BN-based polymer nanocomposites can be prepared, leading to improved thermal conductivity and mechanical strength.[194] Due to their 2D structure, BNNS possess the advantage of easy orientation along the plane within polymer matrices. This characteristic has been leveraged to fabricate nanocomposites with enhanced thermal conductivity using the polymer intercalation method. Song et al.[195] demonstrated the production of composite films by dispersing BNNS in polymers, resulting in nanocomposites with excellent thermal transport performance comparable to polymer/graphene nanocomposites. Similarly, Morishita et al.[196] developed NF-BNNS/thermoplastic polymer composite films through a straightforward wet-process method. NF-BNNS were exfoliated from h-BN by physically adsorbing chlorosulfonic acid on the h-BN surfaces via sonication. The NF-BNNS were then dispersed in acetone and mixed with a poly(methyl methacrylate)/acetone solution. The nanocomposite film was obtained by spreading the solution onto a glass support.

Furthermore, employing the same strategy of nanofiller alignment, poly(vinylidene fluoride-chlorotrifluoroethylene) (P(VDF-CTFE)) nanocomposites with BNNS oriented in parallel within the polymer matrix were prepared by casting. Initially, h-BN was exfoliated using fluoro-hyperbranched polyethylene-*graft*-poly(trifluoroethyl methacrylate) as a polymer stabilizing agent to prevent nanosheet aggregation. The resulting BNNS were then dispersed in dimethylformamide and added to a P(VDF-CTFE) matrix, leading to the formation of BNNS/P(VDF-CTFE) nanocomposite films. To further control the nanosheet orientation along the direction of deformation, the films were uniaxially stretched at a constant temperature (Figure 18).[197] This approach allows for the manipulation of nanosheet orientation, leading to enhanced properties and tailored performance of the nanocomposite films.

**Table 1. Comparison Between BNNTs and BNNS with Additional Properties**

| sr. no. | properties | BNNT | BNNS |
|---|---|---|---|
| 1 | color | white | white |
| 2 | bonding | covalent bonds with ionic component | covalent bonds with ionic component |
| 3 | electronic structure | 5.0–6.0 eV band gap independent of chirality | 5.0–6.0 eV band gap independent of chirality |
| 4 | mechanical properties | Youngs modulus: 0.784–0.912 TPa; 0.71–0.83 TPa (theoretical) | 2D elastic modulus: 22–510 Nm$^{-1}$ (with thickness up to 1–2 nm) |
| 5 | thermal conductivity (WmK$^{-1}$) at room temperature | single wall: 180–300multi wall: 180–300 | 300–2000 theoretical 40 experimental |
| 6 | thermal stability | high up to 800–900 °C in air | superior to graphene |
| 7 | wetting properties and hydrophobicity | poor | water repelling, anticorrosive, and self-cleaning properties |

## 4. PROPERTIES OF BNNT AND BNNS REINFORCED POLYMER NANOCOMPOSITES

Isentropic and Homogenous reinforcing of fillers into matrix polymers requires thorough dispersion of the fillers with no coagulation for even stress distribution for which mixing of the fillers in the matrix polymer becomes a crucial step. For filler reinforcement the critical area of evaluation is the boundary between the reinforcement and the matrix polymer. This region is where the stress transfer from the matrix polymer takes place to the filler and depending on the adhesion between the two this can lead to an isotropic material with a better interfacial interaction and dispersibility. In the case of immiscible materials like BNNTs additional functionalization is required for an appropriate adhesion between the matrix polymer and this filler.

Functionalizing BNNTs by covering them with amine terminated oligomeric polyethylene glycol (PEG1500N)[198] or poly[m-phenylenevinylene-co-2,5,-dictoxyp-phenylenevinylene) (PmPV).[73] An electrostatic interaction between Boron with amine sites in the case of PEG1500N is observed whereas interaction between PmPV with the π stacking present on the surface of BNNTs have proved relatively weak but one in which the interaction can be channelized for various applications. This functionalization has proved to improve the dispersibility of BNNTs across the matrix polymers with a better and stronger interfacial interaction.[45,148] This has further led to improving the overall properties of the matrix polymers with BNNTs as the reinforcements. A study of the molecular dynamics of BNNTs functionalized with PmPV reinforced polystyrene (PS) and polythiophene (PT) shows better and stronger molecular interactions than CNTs in the same.[199−201]

BNNS have shown high miscibility with various solvents thereby reducing the requirement for additional functionalization before utilizing them in polymer applications. There are additional functional groups attached to them which increase their dispersibility when dispersed via sonication. h-BN, the parent material for the majority of all derivatives, exhibits exceptional mechanical properties thereby imparting the same to the derivatives BNNS and BNNTs, making them a suitable option for mechanical reinforcements. Addition of 1% of BNNTs to polystyrene by weight increases the mechanical strength by 7%. These can be further enhanced by using PmPV as a surfactant.[45]

A few parameters were observed wherein the dispersibility of BNNTs, interfacial interactions between the polymer, and the transparency of the polymer seems to be affected directly by the percentage of BNNTs added.

Properties achieved by BNNS, however, depend on the thickness of the BNNS achieved. The most common method of preparation is via exfoliation of h-BN powder and further using sonication centrifugation technique[202] to fabricate various BNNS based transparent composites. Addition of 0.3% BNNS by weight to PMMA increased the strength by 11% and elastic modulus by 22%. Creating a colloidal solution in various solvents was tested[103] which with the addition of just 0.12% by weight increased the properties of PVA by 40% in comparison to the pure polymer. In addition to this, various factors affect the properties imparted to the polymers by BNNS. Uniaxial drawing, strain induced exfoliation, method of preparation of BNNS, and the alignment of the BNNS are just some of the factors which directly increase the efficiency of the mechanical reinforcement especially in case of BNNS.[202−204]

Thermal conduction with electrical insulation is an exceptional property possessed by h-BN materials and their derivatives, which makes them an apt choice for thermally conductive insulating polymer composites. The nano derivatives of h-BN form an advantageous option for reinforcing polymers (the values of the same are discussed in Table 1). Exceptional properties are observed along the lattice plane (002) which exhibits very high thermal conductivity, whereas the thermal conductivity in the other lattice plane is not the same, leading to high thermal conductivity in h-BN. This effect is additionally maximized when the size is in nanometers, as the thickness of the low thermal conducting lattice planes can be reduced. The small size may encourage connection between two particles forming a conductive pathway thereby increasing the thermal conduction in the polymer itself.

PVF composite film with BNNTs 10% by weight can increase the thermal conductivity of the polymer up to 250%.[205] Similar experiments were conducted by incorporating BNNS manufactured by sonication exfoliation and exfoliating h-BN to give nano BNNS in PMMA[34] and PVA. BNNS exfoliated via ball milling, with urea as the solvent are functionalized BNNS as they possess improved stability while dispersing in an aqueous solution.[206] Reduction in the coefficient of thermal expansion was observed. It is extremely important to increase the dispersibility interaction between the filler and the polymer, especially at the grain boundary of the filler. This affects the thermal conductivity of the polymer composite in addition to the size and shape. The interaction can be increased by adding a surface modification for any filler loading.[205,207−210] To improve the homogeneity along a particular direction, the filler orientation and alignment play a very important role. Various processing methods help in increasing the orientation and alignment of the filler, including the electric field application and the magnetic field application in the case of BNNS.[211−214] Whereas in the case of BNNTs,

polymer composite fibers can be aligned during the fabrication process via electrospinning.[215]

Many experiments have also established a correlation between the thermal diffusivity and the alignment of entrenched BNNS in nanocomposites which is valid when the percentage of BNNS added is higher than 10% by weight[216] (Figure 19). Some of the other researchers have also
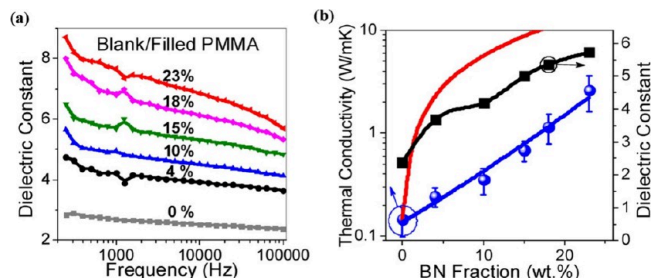
**Figure 19.** (a) Dielectric constants varying with frequency for pure PMMA and PMMA/BN composite materials. (b) The dielectric constant (measured at $10^6$ Hz) and thermal conductivity show an increasing trend as the BN fraction in PMMA/BN composites increases. The blue curve represents the fit to experimental data using the Agari model, while the red curve indicates the theoretical upper limit of thermal conductivities according to a parallel model. Adapted/reprinted with permission from ref 176. Copyright (2012) Springer.

suggested the presence of defects induced during exfoliation of BNNS have proved favorable. These BNNS when incorporated as fillers improve the dispersion of filler in the matrix polymer by reducing the thermal resistance offered by the matrix polymer to BNNS at the interface.[99,217,218]

## 5. APPLICATIONS OF NANOCOMPOSITES IN VARIOUS SECTORS

BN nanocomposites are employed to augment the strength and toughness of the matrix material, creating materials that combine the advantageous properties of both components. In the following sections, we will review the key applications of nanostructured BN and BN-based nanocomposites, with a specific focus on their significance in the fields of energy, environment, and health.

**5.1. Energy Applications.** *5.1.1. Transistors and LED.* This is in terms of Thermal Management wherein BN-based nanocomposites are utilized in electronic devices, such as transistors and LEDs, to enhance thermal conductivity and dissipate heat efficiently. Due to its exceptional thermal properties, BN has garnered significant attention in research for the development of innovative nanocomposites. Single-layer h-BN possesses an impressive theoretical thermal conductivity of approximately 1700 to 2000 $Wm^{-1} K^{-1}$.[10] High power electronic devices face the issue of excessive heat generation at the junction thereby reducing the efficiency and lifespan of the device. A recent study has suggested that utilizing BNNTs as a filler reduces the heat generation as their thermal conductivity is high thereby these acts as a heat sink source.[219]

Reducing the size of field effect transistors (FET) have faced a lot of shortcomings like current leakage, high contact resistance, etc.[220] This was resolved by incorporating BNNTs in FETs without using any semiconductor material. This was achieved by creating a quantum tunnel between BNNT

decorated gold quantum dots.[221] Additionally, iron nanoparticles coated with BNNTs were also utilized providing flexible tunnelling channel with bending angles up to 75°.[222] Exploiting the tubular shape of the BNNTs researchers have filled atomic chains inside with tellurium. These tellurium atoms are covalently bonded with each other inside the chain and stacked on one another using van der Walls forces. The experimentation successfully proved the FET channelling of length up to 100 nm and are therefore categorized as semiconducting materials with high ampacity (Figure 20).[220,223]
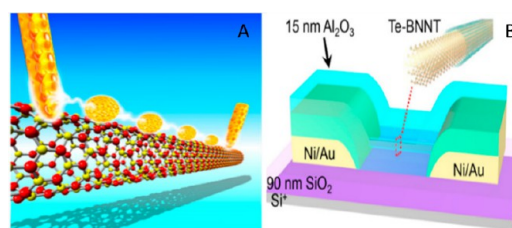
**Figure 20.** (a) Transistors formed by connecting atomic chains inside BNNTs and (b) transistors formed without using semiconductors. Adapted/reprinted with permission from ref 220. Copyright (2021) ACS Publications.

Channelizing the evenness and atomically smooth surfaces and the presence of free dangling bonds and charge traps on the surface of 2 D h-BN, many researchers have experimented with these materials for FET devices for high mobility.[224] One of the researchers fabricated in plane and vertical graphene/h-BN heterostructure device for FET via benzoic acid resulting in electron and holes in graphene 15 000 $cm^2V^{-1}s^{-1}$ at room temperature.[225] Whereas a monolayer h-BN film formed via PECVD at 500 °C for the graphene/h-BN FET device reveals exceptional quality and even multilayer graphene/h-BN films are favorable for FET applications.[224,226]

*5.1.2. Energy Storage and Capacitors.* BNNS have seemed to find their way into sustainable yet efficient energy storage devices like dielectric capacitors, electrochemical capacitors, and commercial batteries. Dielectric capacitors are one of the most preferred due to their high power density, larger operating voltage, and better life with more efficiency. The recent advancements in the field of dielectric capacitors using poly(vinylidene fluoride) (PVDF) as the dielectric film and by further incorporating BNNS into the polymer composite not only increases the dielectric strength but also the overall performance of the capacitor. The $E_b$ value reported is as high as ~1200 $MVVm^{-1}$ with a very low dielectric loss (~2.5 × $10^{-4}$) and excellent electrical insulation. BNNS was added to many more polymers like ferroelectric terpolymer, cross-linked divinyltetram-ethyldisiloxane-bis(benzocyclobutene), reporting excellent results. Therefore addition of BNNS-added polymers to form nanocomposites delivers better overall efficiency than ceramics.[224]

*5.1.3. Thermal Energy.* In nanocomposites, the improvement in thermal conductivity is achieved by minimizing the interfacial thermal resistance between the nanofillers and the polymer or ceramic matrices. By reducing this resistance, heat transfer within the nanocomposite becomes more efficient, leading to enhanced thermal conductivity.[227,228] Notably, the thermal conductivity of nanocomposites depends on factors such as the type of polymer matrix used, and the concentration of fillers incorporated. Optimizing these parameters is crucial

for tailoring the thermal properties of the nanocomposite material to meet the specific application requirements.

PVA/BN films have been found to exhibit higher thermal conductivities at lower BN loads compared to epoxy/BN composites, as demonstrated in the study conducted by Song et al.[195] This finding has sparked further research interest in utilizing PVA as a potential polymer matrix for BN nanocomposites. For instance, Zhang et al.[229] developed h-BN/PVA composites using a vacuum filtration technique, followed by wetting the PVA. During the wetting process, some h-BN fillers diffuse through the polymer matrix, creating pathways for heat conduction. This diffusion phenomenon reduces the time needed for polymer infiltration and, in turn, enhances the thermal conductivity of the resulting nano-composite. This research showcases the potential of PVA as an effective polymer matrix for BN nanocomposites, where the unique interaction between PVA and BN fillers can lead to improved thermal properties which can be a great choice for batteries, electronic chips, mechanical and automotive cooling systems, and 5G.

*5.1.4. Solar Cells.* Nanocomposites play a significant role in enhancing the multifunctionality and efficiency of solar cells, serving as protective and photoactive layers or as surfaces for solar panels.[184] Introducing few-layered h-BN between graphene and *n*-Si has been shown to enhance the performance of Gr/Si Schottky junction solar cells. h-BN acts as an effective electron-blocking and hole-transporting layer, reducing inter-face recombination and improving cell performance.[230]

Perovskites have emerged as promising materials for solar cells due to their high absorption coefficients and process-ability at low temperatures.[232] However, their main drawback lies in their poor environmental stability.[233] Encapsulating perovskites using h-BN materials can greatly improve their stability. Seitz et al.[234] evaluated double-sided encapsulation with h-BN (h-BN/perovskite/h-BN) to provide long-term stability to 2D perovskites based on phenethylammonium lead iodide. By leveraging the insulating behavior and inertness of h-BN, heterojunction solar cells have been developed. Cho et al.[231] prepared $MoS_2$/$WSe_2$ heterojunction solar cells with an h-BN passivation layer using a polydimethylsiloxane (PDMS)-mediated deterministic transfer process. The power conversion efficiency of their h-BN/$MoS_2$/$WSe_2$ heterojunction solar cells (Figure 21) was improved by approximately 74% compared to unmodified h-BN material. This improvement was attributed to the reduced recombination rate at the junction and surface of the semiconductor regions, leading to enhanced overall solar cell performance.

*5.1.5. Hydrogen Storage.* Hydrogen ($H_2$) is a highly attractive renewable energy resource, but its generation and storage for practical applications remain challenging.[235] Low-dimensional BN nanophase materials have shown significant promise in $H_2$ uptake capacity due to their strong interactions with heteropolar BeN bonds and partial $H_2$ chemisorp-tion.[236,237] Highly porous BN microbelts have been synthe-sized through a one-step, template-free reaction between boric acid-melamine precursors and ammonia at moderate con-ditions. These microbelts possess a high specific surface area of 1488 $m^2 g^{-1}$. $H_2$ sorption analysis demonstrated that BN microbelts exhibit reversible $H_2$ uptake ranging from 1.6 to 2.3 wt % at 77 K and relatively low pressure (1 MPa).[238]

Salameh et al.[239] has developed mesoporous monolithic (3D) BN structures using a template-assisted PDC (polymer-derived ceramics) route. These BN monoliths feature a
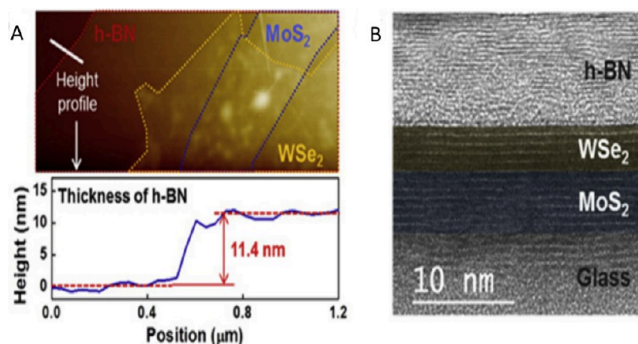


**Figure 21.** (A) Top, AFM image of the $MoS_2$/$WSe_2$/h-BN heterostructures. This image allows for a nanoscale visualization of the arrangement and morphology of the materials in the heterostructure. (B) False-color high-resolution TEM image that illustrates the cross-section of the heterostructure. This image offers detailed insights into the atomic arrangement and interfaces between the $MoS_2$, $WSe_2$, and h-BN layers, providing a clear view of their stacking arrangement and crystal structure. Adapted/reprinted with permission from ref 231. Copyright (2019) ACS Publications.

mesoporous network with a specific surface area ranging from 584 to 728 $m^2 g^{-1}$ and display gravimetric $H_2$ storage capacity of up to 8.1%. Furthermore, BN nanocomposites have potential applications in $H_2$ production. Methods have been developed to increase $H_2$ production using different sources, such as photocatalysis or electrocatalysis[240,241] (Figure 22).

Hydrogen storage affinity was observed by Ti/BNNT as the binding energies of both is similar. Ti can attach up to 7 hydrogen molecules in the quasi-molecular form as Ti is catatonically functionalized and B−N surface bonds are heteropolar in nature.[242] It has been observed that BNNTs can take up to 2.6% of dopants, defects, or any surface imperfections which might aid improvement in the electrical properties.[243,244] This can be achieved when BNNTs defect sites are modified with a transition metal specifically for hydrogen storage. Ti dopants can modify the electronic properties of BNNTs by affecting their charge transfer behavior.[242,245]

*5.1.6. Electrochemical Devices.* BN-based nanocomposites have emerged as an interesting choice for use in electro-chemical devices.[246] Researchers like Idrees et al. and Wan et al.[247,248] have focused on polymer-derived ceramics (PDC)-based nanocomposites as stable electrodes for Li-ion batteries (LIB) and other electrochemical applications. The combina-tion of PDCs with other nanomaterials, such as carbon nanotubes,[249,250] graphite,[251] and BN,[252] leads to structural modifications that enhance their properties, making them promising candidates for potential applications in LIB and supercapacitors. For instance, David et al.[252] demonstrated that integrating exfoliated BNNS into SiCN (silicon carboni-tride) significantly increases the charge capacity of free-standing SiCN-based LIB electrodes. Similarly, Singh et al.[253] investigated how Li+ insertion capacity could be enhanced by incorporating various loads of BNNTs into SiOC (silicon oxycarbide) ceramics. The presence of BNNTs in the composite affected the free carbon phase within the SiOC matrix, resulting in improved electrochemical performance.

The versatility and tunability of BN-based nanocomposites make them attractive for developing advanced electrode materials with enhanced electrochemical properties, paving the way for more efficient and durable electrochemical devices.
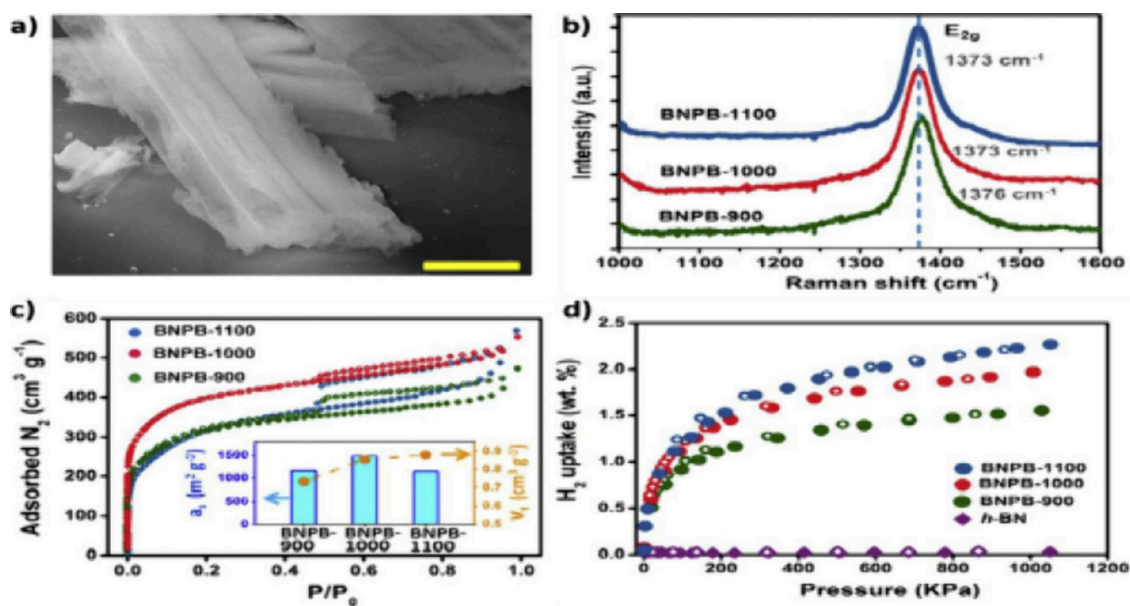
**Figure 22.** (a) Tilted view of isolated porous structures, clearly revealing the belt-shaped morphology of the BN micro belts. The scale bar indicates a length of 1 mm, giving an idea of the size of the structures. (b) Raman spectra of BN porous micro belts prepared at different temperatures, namely 900 °C, 1000 °C, and 1100 °C. Raman spectroscopy provides information about the structural and chemical characteristics of the BN micro belts. (c) Nitrogen adsorption−desorption isotherms of BN porous micro belts prepared at the same temperatures mentioned earlier. These isotherms provide insights into the porosity and surface area of the BN micro belts. The inset in this panel summarizes the Brunauer−Emmett−Teller (BET) surface areas and total pore volumes for the obtained samples. (d) $H_2$ adsorption−desorption isotherms of the BN porous micro belts at 77 K and 1 MPa. This data showcases the $H_2$ uptake capacity of the BN micro belts under specific conditions. Adapted/reprinted with permission from ref 238. Copyright (2013) ACS Publications.
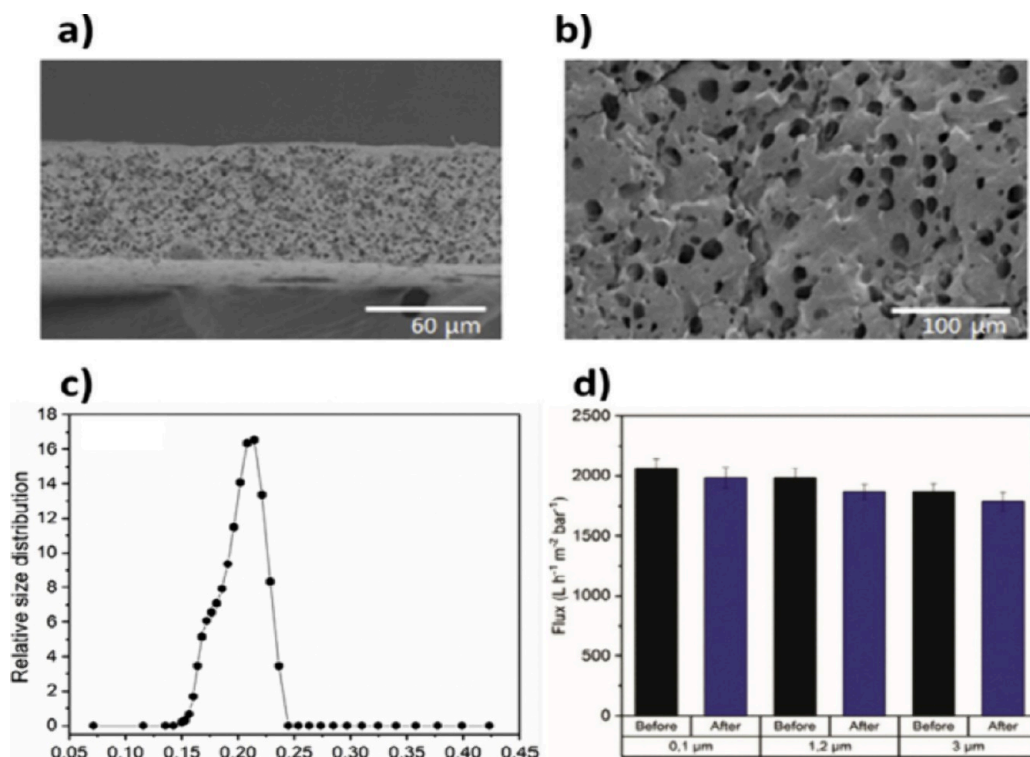


**Figure 23.** (a) View of the cross-section of the h-BNNS/PVA membrane nanocomposite. It reveals the internal structure and layering of the membrane (b) Surface SEM photograph displaying the top view of the h-BNNS/PVA membrane nanocomposite, providing insight into the morphology and surface characteristics of the material. (c) Plot representing the relative pore size distribution of the h-BNNS/PVA membrane. It gives information about the distribution of pore sizes within the nanocomposite membrane (d) Corresponding flux values of the h-BNNS/PVA membrane nanocomposite before and after conducting particle rejection tests. Flux is the rate of fluid flow through the membrane, and the tests are performed to evaluate the membrane's effectiveness in rejecting particles from the fluid. Adapted/reprinted with permission from ref 28. Copyright (2018) RSC Publications.

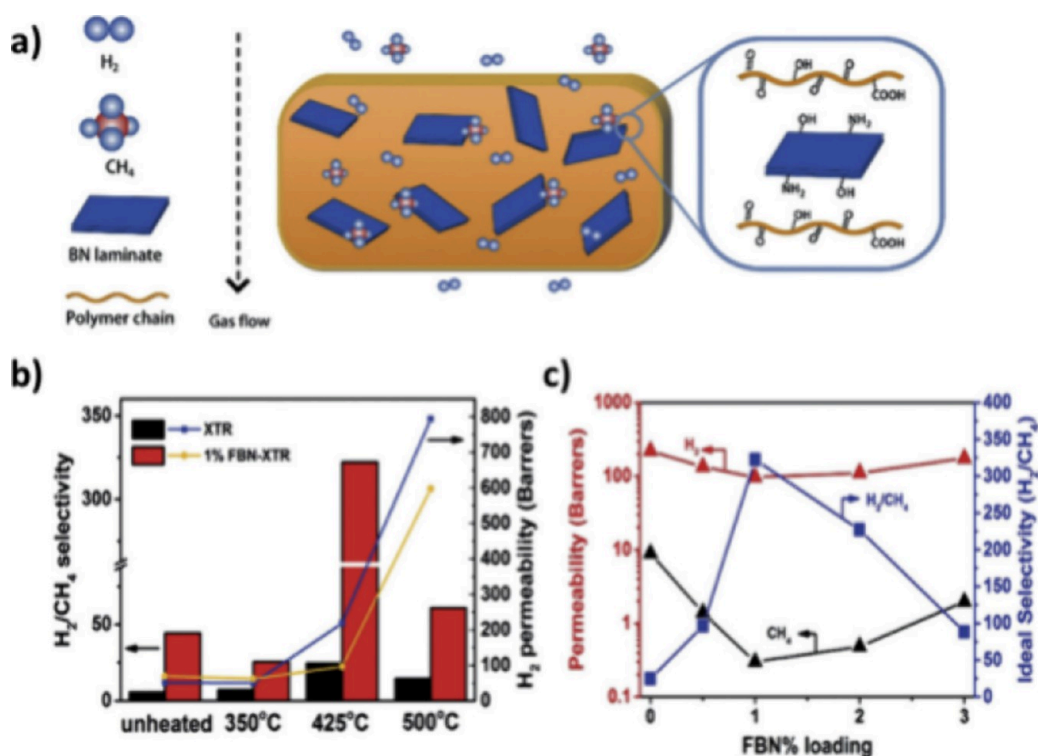**Figure 24.** (a) Schematic representation of the FBN-XTR membrane structure and the process of selective gas permeation through the membrane. This provides an overview of how the membrane functions in separating different gases. (b) $H_2$ permeability and $H_2/CH_4$ selectivity of 1 wt % FBN-XTR and pure XTR membranes at different thermal rearrangement temperatures. It shows the relationship between the membrane composition and gas separation performance. (c) Gas permeability and selectivity of membranes with various FBN loads, specifically for the $H_2/CH_4$ gas pair, at a temperature of 258 °C and pressure of 1 bar. It demonstrates how the gas separation performance varies with different FBN loadings in the membrane. Adapted/reprinted with permission from ref 261. Copyright (2018) Wiley online library.

**5.2. Environmental Applications.** *5.2.1. Water Purification.* Environmental applications are available in terms of water purification wherein BN nanocomposites are used in filtration systems for efficient water purification, owing to their high surface area and tunable porosity. Novel BN-based materials have shown great potential for applications in water technologies, especially in water purification processes. BN nanotubes (BNNTs) have exceptional adsorption properties, making them highly effective for sorbing pollutants like oil and organic solvents from heavy industries and for water purification.[254−256]

Researchers have also fabricated BN-based nanocomposites specifically for water purification using templating methods. Gonzalez Ortiz et al.[28] developed innovative h-BN nanosheet (h-BNNS) and poly(vinyl alcohol) (PVA) based nanocomposites. They created porous membranes by casting a homogeneous h-BNNS/PVA dispersion onto a glass support, followed by coagulation in a water bath to remove the solvent and form the porous structure. The h-BNNS/PVA nanocomposite membranes were then tested for permeability to pure water and particle rejection (Figure 23). The results showed high pure water permeability values of approximately 2000 L h$^{-1}$ m$^{-2}$ bar$^{-1}$ and a rejection efficiency of around 76% for particles of about 0.1 mm in size. BN-based nanocomposites offer promising solutions for efficient water purification, providing opportunities for addressing environmental challenges and advancing water treatment technologies.

*5.2.2. Gas Separation.* Gas separation technologies play a crucial role in chemical industries due to their clean and energy-efficient nature, along with high transport selectiv-

ity.[257,258] Nanocomposites made from polymeric materials have garnered extensive research attention due to their numerous advantages, including being lightweight, having process flexibility, and being cost-effective.[259] The potential applications of hexagonal boron nitride (h-BN) in gas separation have been theoretically explored, particularly for separating $H_2$ and $CH_4$ gases. h-BN has demonstrated excellent $H_2/CH_4$ selectivity (>105 at room temperature) and low adsorption energies (around 0.1 eV) for both $H_2$ and $CH_4$ on monolayer membranes.[260] This makes h-BN an attractive candidate for gas separation applications. In practice, functionalized BN nanosheets (FBN) have been incorporated as fillers in thermally rearranged polyimide (XTR) to tailor the gas transport and mechanical properties, resulting in an FBN-XTR nanocomposite (Figure 24). FBN-XTR membranes have been employed for $H_2$ separation, showing superior $H_2/CH_4$ separation performance compared to state-of-the-art membranes.[261]

By leveraging the unique properties of h-BN and incorporating it into polymeric matrices as nanocomposites, researchers are paving the way for the development of advanced gas separation membranes with improved selectivity and efficiency in chemical industries.

**5.3. Applications in Field of Heath.** BN nanocomposites show great promise in advancing technologies and addressing challenges in these critical areas, making significant contributions to the energy sector, environmental sustainability, and advancements in healthcare. Their stability, flexibility, size, shape, low toxicity, and biodegradability make BN an ideal candidate for nanocarriers. For efficient drug delivery,
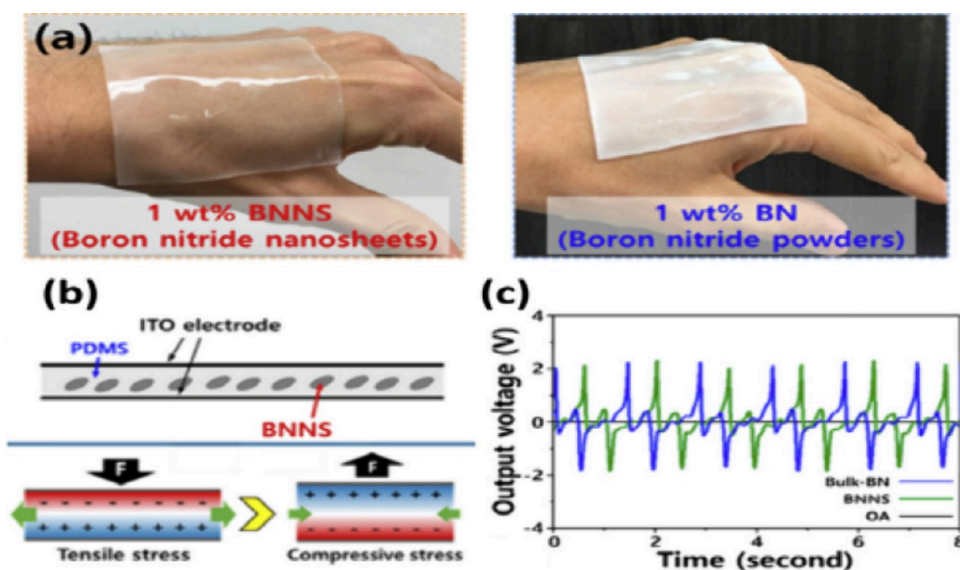
**Figure 25.** (a) Transparent BNNS with I% BNNS by weight addition and addition of Boron nitride by 1% by addition by weight. (b) Mechanism of TFPS design. (c) Voltage signals of BNNS, h-BN, and OA samples utilized in a PDMS composite device with mechanical vibration infused. Adapted/reprinted with permission from ref 266. Copyright (2018) Science Direct.

nanoparticles should be small enough to travel through blood vessels and penetrate tissues, while also being large enough to avoid being filtered out through endothelial fenestrations (pores in the endothelial cells of blood vessels). BN nanoparticles can be synthesized in various sizes, allowing for optimization of drug loading and delivery.[262]

By leveraging these characteristics, BN nanocomposites can be engineered to transport and release therapeutic agents effectively, offering a promising avenue for targeted drug delivery and improved treatments in the medical field. The advancement of sensing technologies, particularly wearable biomedical electronic devices, and novel sensing functionalities like fluorescence or colorimetric detection methods, has witnessed rapid growth in recent years. Consequently, there is a significant focus on designing and producing functional nanocomposite materials with specific physicochemical properties to create sensors, leading to a prominent area of research.[263]

In the pursuit of new sensing functionalities, researchers have developed nanosized copper sulfide (CuS) dispersed on the surface of BN nanosheets (BNNS-CuS) through a straightforward solvothermal process. This unique sensing material, BNNS-CuS, has been utilized for the visual detection of total cholesterol in human serum. The study demonstrated that BNNS-CuS devices exhibit high selectivity toward cholesterol, with a linear detection range of 10 to 100 mM and a detection limit as low as 2.9 mM.[264]

These findings showcase the potential of BN nanocomposites in sensor development and their ability to offer precise and sensitive detection capabilities for various applications, including biomedical sensing and diagnostics. Biomedical imaging can be done by BN nanocomposites. These are utilized as contrast agents in biomedical imaging techniques, enabling enhanced imaging and diagnostics. BN-based nanocomposites are explored for drug delivery applications, facilitating targeted and controlled drug release.

BNNS have great potential for use as reinforcement in nanocomposite materials or scaffolds for tissue engineering and regenerative medicine. This is due to their ability to improve the mechanical and thermal properties of the materials without adversely affecting the properties of the polymer used. A study conducted by Nagarajan et al.[265] involved the synthesis of gelatin/h-BNNS bionanocomposites through the process of electrospinning. Subsequently, the nanocomposites were cross-linked to enhance their stability in aqueous media. The use of BNNS in such bionanocomposites can significantly enhance the overall properties of the materials, making them well-suited for tissue engineering applications where mechanical integrity and biocompatibility are critical factors. By combining BNNS with biocompatible polymers like gelatin, researchers are paving the way for innovative approaches in regenerative medicine and tissue repair. These advancements hold great promise for the development of novel biomaterials that can promote tissue regeneration and healing (Figures 25 and 26).

**5.4. Radiation Absorption and Neutron Shielding.** Whenever cosmos radiation interacts with any matter in space it leads to the generation of neutrons which further lead to the destruction of the space equipment and can also damage the health of astronauts. NASA has shown that an isotope of $^{10}$B
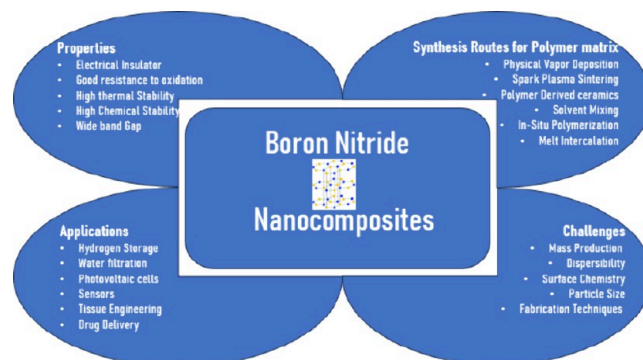


**Figure 26.** An overview of the current obstacles faced by BN nanocomposites, including the types and properties of BN nanostructures, approaches for synthesizing polymer- and ceramic-based nanocomposites, and their diverse applications and potential opportunities.

formed BNNTs when incorporated in a polyamide film composite increases the neutron absorption by 120%.[267] Hydrogen containing nanotubes are a recent area of research interest as they improve the radiation shielding from solar particle events and galactic cosmic radiation.[268] They have shown a higher affinity to store zero dimensional particles due to their high hydrogen binding energy and high surface area.[269−274]

## 6. CONCLUSIONS AND FUTURE OUTLOOK

1D and 2D h-BN nanostructures have promising applications in various fields. The growth of high quality and bulk production is still a challenge. h-BN composites with other materials have evolved rapidly because their performance and properties can be tailored. The research incorporating h-BN nano derivatives to form polymer composites is still in its nascent stage whereas the results of the same have proved to be extremely promising.

There are many difficulties observed in the preparation, structural analysis, and parameters measurements of BNNTs. The first BNNT was discovered almost 25 years ago but only over the past decade has significant work been observed. For any mass applications of BNNTs the yield and the purity form the most critical hurdle that must be overcome by the researchers of today. Many routes of synthesis through which BNNTs can be synthesized are discussed above. They form the perfect filler as they have an added advantages of electrically insulating properties, high resistance to oxidation, and much more as discussed above.

An additive advantage in terms of BNNS can be achieved with liquid exfoliation of h-BN for mass production which can be incorporated in polymer composition, but the yield and thickness is still a concern. A recent advancement yielding an increased filler fraction of BNNS has led to very high in-plane thermal conductivity in polymer composites. This property is a directional property which makes the thermal conductivity in the perpendicular direction of the filler alignment very low. One of the vast and most unexplored areas of interest are the solvents of exfoliation. Since all the methods mostly involve the use of solvents many researchers can focus on the criteria of dispersion, and furthermore, the sample selected from a nonhomogeneously dispersed solvent leads to inaccurate experimentation. BNNS can form stable solutions rather than precipitates but is not correlated to the well dispersion, defects in the layers, or any other details related to the exfoliation process. The additional validation of the results is usually done by TEM where the sample created is so small with only a ew BNNS present at the cross-section. Therefore, this extensive experimental validation may make comparing the data received by XRD and the multiple nanoscale images of the TEM with the bulk results based on assumption. Attaching hydroxl groups on the boron end, reacting them with the hydroxl group, and then hydrogenating the nitrogen group and further reacting it with the amino group improves the dispersibility of the fillers in the nanocomposites.

A varied area of research in terms of BN nanostructures has not been utilized, therefore considering the availability of utilizing BNNS, due to their similar properties to BNNTs and better availability, BNNS incorporated polymer nanocomposites may represent a preferable option for researchers to use in the areas of optical properties, transparent polymers, radiation properties, biocompatibilities, electronic packaging, thermal management of energy, hydrogen fuel cells, photovoltaic

packaging, and many more. There are many methods of making these nanocomposites but selecting the appropriate method and fine-tuning it is crucial, depending on the specific target application, composition, and dispersion requirements. Achieving a uniform dispersion of nanofillers within polymer matrices is a fundamental prerequisite for obtaining the desired mechanical and physical characteristics in nanocomposites. The properties of these nanocomposites are also influenced by the chemistry of the polymer matrix and the nature of the nanofillers used. The interfaces between the polymer matrix and nanofillers can significantly impact the effectiveness of load transfer. Therefore, surface functionalization of nanofillers plays important role in improving their dispersion and enhancing the interfacial adhesion between the matrix and fillers, thereby optimizing the overall performance of the nanocomposite material, a key factor toward high performing nanocomposites.

There are a few challenges which can be observed in the journey of BN nanostructures, namely the lack of mass production of these structures as all of these results have proved to be extremely successful, making these materials very expensive. The materials have not been fully explored due to the mass production issues. This further leads to limitations in testing when it comes to experimentation and iterating the percentage of fillers to check for properties at various stages. The percentage addition of BN nanostructures above 5% by weight has also shown agglomeration at various sites of the polymer, leading to anisotropic properties in terms of thermal, mechanical, electrical, etc. Moreover, this also leads to poor interfacial properties among the fillers and polymer composite. The ionic bond of B−N elements restricts the initiation of chemical reactions in the case of any surface modification. Furthermore, the distribution of 1D and 2D nano structures among the other materials like polymers is critical. The grain boundary condition between the filler and the polymer at the interface and a homogeneous distribution of the fillers throughout the polymers are the primary conditions to produce BN nanostructure incorporated polymer composites. The selection of the exfoliation process and the quality of BNNS depends on the application. There are a few applications which may allow leverage for slight defects. There are shortcomings related to the validation of BNNS via XRD and TEM wherein the intricate exfoliated BNNS mixtures lead to either peak broadening or even shifting of the peak depending on the quality of exfoliation. With all the review articles referred to in this paper, a crucial challenge identified for the researchers working in the field of BNNS and BNNTs is to define a set of parameters which defines what high quality nanomaterials are by creating a benchmark. This can be shared across the community, making reproduction of the results easier via modifying exfoliation processes and processing parameters. Thus, these also act as the future areas wherein researchers can explore the range of work.

## ■ AUTHOR INFORMATION

### Corresponding Author

Dattatray J. Late − Centre of Nanoscience and Nanotechnology, Amity School of Engineering and Technology, Amity University Maharashtra, Mumbai, Maharashtra 410206, India; orcid.org/0000-0003-3007-7220; Email: datta099@gmail.com, djlate@mum.amity.edu

## Authors

**Gunchita Kaur Wadhwa** − *Centre of Nanoscience and Nanotechnology, Amity School of Engineering and Technology, Amity University Maharashtra, Mumbai, Maharashtra 410206, India;* ⓘ orcid.org/0000-0003-1233-8407

**Shrikant Charhate** − *Amity School of Engineering and Technology, Amity University Maharashtra, Panvel, Mumbai, Maharashtra 410206, India*

**Shashi Bhushan Sankhyan** − *Centre of Nanoscience and Nanotechnology, Amity School of Engineering and Technology, Amity University Maharashtra, Mumbai, Maharashtra 410206, India*

Complete contact information is available at:
https://pubs.acs.org/10.1021/acsomega.3c10217

## Notes

The authors declare no competing financial interest.

## ■ REFERENCES

(1) Sinha Ray, S.; Okamoto, M. Polymer/layered silicate nanocomposites: a review from preparation to processing. *Prog. Polym. Sci.* **2003**, *28*, 1539.

(2) Stankovich, S.; Dikin, D. A.; Dommett, G. H. B.; Kohlhaas, K. M.; Zimney, E. J.; Stach, E. A.; Piner, R. D.; Nguyen, S. B. T.; Ruoff, R. S. Graphene-based composite materials. *Nature* **2006**, *442*, 282.

(3) Clifton, S.; Thimmappa, B. H. S.; Selvam, R.; Shivamurthy, B. Polymer nanocomposites for high-velocity impact applications-A review. *Compos. Commun.* **2020**, *17*, 72.

(4) Kuila, T.; Srivastava, S. K.; Bhowmick, A. K.; Saxena, A. K. Ethylene vinyl acetate/ethylene propylene diene terpolymer-blend-layered double hydroxide nanocomposites. *Compos. Sci. Technol.* **2008**, *68*, 3234.

(5) Hong, C. E.; Lee, J. H.; Kalappa, P.; Advani, S. G. Preparation and properties of reduced graphene oxide/polyacrylonitrile nanocomposites using polyvinyl phenol. *Compos. Sci. Technol.* **2007**, *67*, 1027.

(6) Li, P.; Kim, N. H.; Hui, D.; Rhee, K. Y.; Lee, J. H. Solvent-responsive polymernanocapsules with controlled permeability: encapsulation and release of a fluorescent dye by swelling and deswelling. *Appl. Clay Sci.* **2009**, *46*, 414.

(7) Bee, S.-L.; Abdullah, M. A. A.; Bee, S.-T.; Sin, L. T.; Rahmat, A. R. Polymer nanocomposites based on silylated-montmorillonite: A review. *Prog. Polym. Sci.* **2018**, *85*, 57.

(8) Camargo, P. H. C.; Satyanarayana, K. G.; Wypych, F. Nanocomposites: synthesis, structure, properties and new application opportunities. *Mater. Res.* **2009**, *12*, 1−39.

(9) Fu, S.; Sun, Z.; Huang, P.; Li, Y.; Hu, N. Some basic aspects of polymer nanocomposites: A critical review. *Nano Mater. Sci.* **2019**, *1*, 2.

(10) Gonzalez-Ortiz, D.; Salameh, C.; Bechelany, M.; Miele, P. Nanostructured boron nitrideebased materials: synthesis and applications. *Mater. Today Adv.* **2020**, *8*, 100107.

(11) Jiang, X.-F.; Weng, Q.; Wang, X.-B.; Li, X.; Zhang, J.; Golberg, D.; Bando, Y. Recent Progress on Fabrications and Applications of Boron Nitride Nanomaterials: A Review. *J. Mater. Sci. Technol.* **2015**, *31*, 589.

(12) Wang, J.; Ma, F.; Sun, M. Graphene, hexagonal boron nitride, and their heterostructures: properties and applications. *RSC Adv.* **2017**, *7*, 16801.

(13) Zeng, H.; Zhi, C.; Zhang, Z.; Wei, X.; Wang, X.; Guo, W.; Bando, Y.; Golberg, D. 'White graphenes': boron nitride nanoribbons via boron nitride nanotube unwrapping. *Nano Lett.* **2010**, *10*, 5049−5055.

(14) Gonzalez Ortiz, D.; Pochat-Bohatier, C.; Cambedouzou, J.; Bechelany, M.; Miele, P. Exfoliation of hexagonal boron nitride (h-BN) in liquide phase by on intercalation. *Nanomaterials* **2018**, *8*, 716.

(15) Patki, A. M.; Goyal, R. K. High performance polyetherketone-hexagonal boron nitride nanocomposites for electronic applications. *J. Mater. Sci. Mater. Electron* **2019**, *30*, 3899−3908.

(16) Li, Q.; Chen, L.; Gadinski, M. R.; Zhang, S.; Zhang, G.; Li, H. U.; Iagodkine, E.; Haque, A.; Chen, L.-Q.; Jackson, T. N.; Wang, Q. Flexible hig-temperature dielectric materials from polymer nanocomposites. *Nature* **2015**, *523*, 576−579.

(17) Oh, H.; Kim, J. Fabrication of polymethyl methacrylate composites with silanized boron nitride by in-situ polymerization for high thermal conductivity. *Composites Science and Technolgy* **2019**, *172*, 153−162.

(18) Thangaraj, V.; Bussiere, J.; Janot, J. M.; Bechelany, M.; Jaber, M.; Subramanian, S.; Miele, P.; Balme, S. Fluorescence quenching of sulforhodamine dye over graphene oxide and boron nitride nanosheets. *Eur. J. Inorg. Chem.* **2016**, *2016*, 2125−2130.

(19) Weng, Q.; Wang, X.; Zhi, C.; Bando, Y.; Golberg, D. microbelts for hydrogen storage Boron nitride porous. *ACS Nano* **2013**, *7*, 1558−1565.

(20) Naresh Muthu, R.; Rajashabala, S.; Kannan, R. Hexagonal boron nitride (h-BN) nanoparticles decorated multi-walled carbon nanotubes (MWCNT) for hydrogen storage. *Renew. Energy* **2016**, *85*, 387−394.

(21) Farshid, B.; Lalwani, G.; Shir Mohammadi, M.; Simonsen, J.; Sitharaman, B. Boron nitride nanotubes and nanoplatelets as reinforcing agents of polymeric matrices for bone tissue engineering. *J. Biomed. Mater. Res. B Appl. Biomater* **2017**, *105*, 406−419.

(22) Jedrzejczak-Silicka, M.; Trukawka, M.; Dudziak, M.; Piotrowska, K.; Mijowska, E. Hexagonal boron nitride functionalized with Au nanoparticlesdproperties and potential biological applications. *Nanomater.* **2018**, *8*, 605.

(23) Yu, S.; Wang, X.; Pang, H.; Zhang, R.; Song, W.; Fu, D.; Hayat, T.; Wang, X. Boron nitride-based materials for the removal of pollutants from aqueous solutions: A review. *Chem. Eng. J.* **2018**, *333*, 343−360.

(24) Chen, C.; Wang, J.; Liu, D.; Yang, C.; Liu, Y.; Ruoff, R. S.; Lei, W. Functionalized boron nitride membranes with ultrafast solvent transport performance for molecular separation. *Nature Communication* **2018**, *9*, 1902.

(25) Kamble, A. R.; Patel, C. M.; Murthy, Z. V. P. Effects of inorganic additive of two- dimensional hexagonal boron nitride on the gas separation/permeation for PVDF-derived membranes. *Sep. Sci. Technol.* **2019**, *54*, 1489−1501.

(26) Weber, M.; Koonkaew, B.; Balme, S.; Utke, I.; Picaud, F.; Iatsunskyi, I.; Coy, E.; Miele, P.; Bechelany, M. Boron nitride nanoporous membranes with high surface charge by atomic layer deposition. *ACS Appl. Mater. Interfaces* **2017**, *9*, 16669−16678.

(27) Weber, M.; Iatsunskyi, I.; Coy, E.; Miele, P.; Cornu, D.; Bechelany, M. Novel and facile route for the synthesis of tunable boron nitride nanotubes combining atomic layer deposition and annealing processes for water purification. *Adv. Mater. Interfaces* **2018**, *5* (16), No. 1800056.

(28) Gonzalez-Ortiz, D.; Pochat-Bohatier, C.; Gassara, S.; Cambedouzou, J.; Bechelany, M.; Miele, P. Development of novel h-BNNS/PVA porous membranes via Pickering emulsion templating. *Green Chem.* **2018**, *20*, 4319−4329.

(29) Meng, W.; Huang, Y.; Fu, Y.; Zhi, C. Polymer composites of boron nitride nanotubes and Nanosheets. *J. Mater. Chem. C* **2014**, *2* (47), 10049−10061.

(30) Golberg, D.; Bando, Y.; Huang, Y.; Xu, Z.; Wei, X.; Bourgeois, L.; Wang, M.-S.; Zeng, H.; Lin, J.; Zhi, C. Boron nitride nanotubes and nanosheets. *Isr. J. Chem.* **2010**, *50*, 405.

(31) Yu, S.; Wang, X.; Pang, H.; Zhang, R.; Song, W.; Fu, D.; Hayat, T.; Wang, X. Synergistic effect of well-defined dual sites boosting the oxygen reduction reaction. *Energy Environ. Sci.* **2018**, *11*, 3375−3379, DOI: 10.1039/C8EE02656D.

(32) Sharma, V.; Kagdada, H. L.; Jha, P. K.; Spiewak, P.; Kurzydłowski, K. J. Thermal transport properties of boron nitride based materials: A review. *Renew. Sustain. Energy Rev.* **2020**, *120*, No. 109622.

(33) Nagashima, A.; Tejima, N.; Gamou, Y.; Kawai, T.; Oshima, C. Electronic Structure of Monolayer Hexagonal Boron Nitride Physisorbed on Metal Surfaces. *Phys. Rev. Lett.* **1995**, 75, 3918.

(34) Zhi, C. Y.; Bando, Y.; Tang, C. C.; Kuwahara, H.; Golberg, D. Large-Scale Fabrication of Boron Nitride Nanosheets and Their Utilization in Polymeric Composites with Improved Thermal and Mechanical Properties. *Adv. Mater.* **2009**, 21, 2889−2893.

(35) Wang, T.; Wang, M.; Fu, L.; Duan, Z.; Chen, Y.; Hou, X.; Wu, Y.; Li, S.; Guo, L.; Kang, R.; Yu, J. Enhanced Thermal Conductivity of Polyimide Composites with Boron Nitride Nanosheets. *Sci. Rep.* **2018**, 8, 1557.

(36) Iijima, S. Helical microtubules of graphitic carbon. *Nature* **1991**, 354, 56.

(37) Hamada, N.; Sawada, S.-i.; Oshiyama, A. New one-dimensional conductors: Graphitic microtubules. *Phys. Rev. Lett.* **1992**, 68, 1579.

(38) Saito, R.; Fujita, M.; Dresselhaus, G.; Dresselhaus, M. S. Electronic structure of graphene tubules based on C60. *Phys. Rev. B* **1992**, 46, 1804.

(39) Gao, R.; Yin, L.; Wang, C.; Qi, Y.; Lun, N.; Zhang, L.; Liu, Y.-X.; Kang, L.; Wang, X. High-Yield Synthesis of Boron Nitride Nanosheets with Strong Ultraviolet Cathodoluminescence Emission. *J. Phys. Chem. C* **2009**, 113, 15160.

(40) Chopra, N. G.; Luyken, R. J.; Crespi, V. H.; Cohen, M.; Louie, S. G.; Zettl, A. Boron Nitride Nanotubes. *Science* **1995**, 269 (5226), 966−967.

(41) Rubio, A.; Corkill, J. L.; Cohen, M. L. Theory of graphitic boron nitride nanotubes. *Phys. Rev. B.* **1994**, 49, 5081.

(42) Blase, X.; Rubio, A.; Louie, S.G.; Cohen, M.L. Stability and Band Gap Constancy of Boron-Nitride Nanotubes. *Europhys. Lett.* **1994**, 28, 335.

(43) Chen, Y.; Zou, J.; Campbell, S. J.; Le Caer, G. Boron nitride nanotubes: Pronounced resistance to oxidation. *Appl. Phys. Lett.* **2004**, 84, 2430.

(44) Chen, H.; Chen, Y.; Li, C. P.; Zhang, H.; Williams, J. S.; Liu, Y.; Liu, Z.; Ringer, S. P. Eu-doped Boron Nitride Nanotubes as a Nanometer-Sized Visible-Light Source. *Adv. Mater.* **2007**, 19, 1845.

(45) Zhi, C. Y.; Bando, Y.; Tang, C. C.; Honda, S.; Kuwahara, H.; Golberg, D. Boron nitride nanotubes/polystyrene composites. *J. Mater. Res.* **2006**, 21, 2794−2800.

(46) Chopra, N. G.; Luyken, R. J.; Cherrey, K.; Crespi, V. H.; Cohen, M. L.; Louie, S. G.; Zettl, A. Boron Nitride Nanotubes. *Science* **1995**, 269, 966−967.

(47) Loiseau, A.; Willaime, F.; Demoncy, N.; Schramchenko, N.; Hug, G.; Colliex, C.; Pascard, H. Boron nitride nanotubes. *Carbon* **1998**, 36, 743−752.

(48) Loiseau, A.; Willaime, F.; Demoncy, N.; Hug, G.; Pascard, H. Boron Nitride Nanotubes with Reduced Numbers of Layers Synthesized by Arc Discharge. *Phys. Rev. Lett.* **1996**, 76, 4737.

(49) Suenaga, K.; Colliex, C.; Demoncy, N.; Loiseau, A.; Pascard, H.; Willaime, F. Synthesis of Nanoparticles and Nanotubes with Well-Separated Layers of Boron Nitride and Carbon. *Science* **1997**, 278, 653−655.

(50) Cumings, J.; Zettl, A. Mass-production of boron nitride double-wall nanotubes and nanococoons. *Chem. Phys. Lett.* **2000**, 316, 211−216.

(51) Xu, L. Q.; Peng, Y. Y.; Meng, Z. Y.; Yu, W. C.; Zhang, S. Y.; Liu, X. M.; Qian, Y. T. A Co-pyrolysis Method to Boron Nitride Nanotubes at Relative Low Temperature. *Chem. Mater.* **2003**, 15, 2675−2680.

(52) Rosas, G.; Sistos, J.; Ascencio, J. A.; Medina, A.; Perez, R. Synthesis of AlFe Intermetallic Nanoparticles by High-Energy Ball Milling. *Appl. Phys. A: Mater. Sci. Process.* **2005**, 80, 377−380.

(53) Dai, J.; Xu, L. Q.; Fang, Z.; Sheng, D. P.; Guo, Q. F.; Ren, Z. Y.; Wang, K.; Qian, Y. T. Space-selective precipitation of functional crystals in glass by using a high repetition rate femtosecond laser. *Chem. Phys. Lett.* **2007**, 440, 253−258.

(54) Han, W. Q.; Bando, Y.; Kurashima, K.; Sato, T. Structure of chemically derived mono- and few-atomic-layer boron nitride sheets. *Appl. Phys. Lett.* **1998**, 73, 3085−3087.

(55) Golberg, D.; Bando, Y.; Kurashima, K.; Sato, T. Nanotubes of boron nitride filled with molybdenum clusters. *Chem. Phys. Lett.* **2000**, 323, 185−191.

(56) Bechelany, M.; Bernard, S.; Brioude, A.; Cornu, D.; Stadelmann, P.; Charcosset, C.; Fiaty, K.; Miele, P. Synthesis of boron nitride nanotubes by a template-assisted polymer thermolysis process. *J.Phys. Chem. C* **2007**, 111, 13378−13384.

(57) Shimizu, Y.; Moriyoshi, Y.; Tanaka, H.; Komatsu, S. Boron nitride nanotubes, webs, and coexisting amorphous phase formed by the plasma jet method. *Appl. Phys.lett* **1999**, 75, 929−932.

(58) Bengu, E.; Marks, L. D. Single-Walled BN Nanostructures. *Phys. Rev. Lett.* **2001**, 86, 2385−2387.

(59) Golberg, D.; Bando, Y.; Eremets, M.; Takemura, K.; Kurashima, K.; Yusa, H. Nanotubes in boron nitride laser heated at high pressure. *Appl. Phys. Lett.* **1996**, 69, 2045−2047.

(60) Smith, M. W.; Jordan, K. C.; Park, C.; Kim, J. W.; Lillehei, P. T.; Crooks, R.; Harrison, J. S. Very long single- and few-walled boron nitride nanotubes via the pressurized vapor/condenser method. *Nanotechnology* **2009**, 20, No. 505604.

(61) Laude, T.; Matsui, Y.; Marraud, A.; Jouffrey, B. Long ropes of boron nitride nanotubes grown by a continuous laser heating. *Appl. Phys.lett.* **2000**, 76, 3239−3241.

(62) Yu, D. P.; Sun, X. S.; Lee, C. S.; Bello, I.; Lee, S. T.; Gu, H. D.; Leung, K. M.; Zhou, G. W.; Dong, Z. F.; Zhang, Z. Amorphous silica nanowires: Intensive blue light emitters. *Appl. Phys. Lett.* **1998**, 72, 1966−1968.

(63) Arenal, R.; Stephan, O.; Cochon, J. L.; Loiseau, A. Young modulus, mechanical and electrical properties of isolated individual and bundled single-walled boron nitride nanotubes. *J. Am. Chem. Soc.* **2007**, 129, 16183−16189.

(64) Chen, Y.; Chadderton, L. T.; FitzGerald, J.; Williams, J. S. A solid-state process for formation of boron nitride nanotubes. *Appl. Phys. Lett.* **1999**, 74, 2960−2962.

(65) Chen, Y.; Conway, M.; Williams, J. S.; Zou, J. Large-quantity production of high-yield boron nitride nanotubes. *J. Mater. Res.* **2002**, 17, 1896−1899.

(66) Yu, J.; Chen, Y.; Wuhrer, R.; Liu, Z. W.; Ringer, S. P. Boron nitride nanotubes: synthesis and applications. *Chem. Mater.* **2005**, 17, 5172−5176.

(67) Kim, J.; Lee, S.; Uhm, Y. R.; Jun, J.; Rhee, C. K.; Kim, G. M. *Acta Mater.* **2011**, 59, 2807−2813.

(68) Lourie, O. R.; Jones, C. R.; Bartlett, B. M.; Gibbons, P. C.; Ruoff, R. S.; Buhro, W. E. *CVD Growth of Boron Nitride Nanotubes* **2000**, 12 (7), 1808−1810.

(69) Tang, C.; Bando, Y.; Sato, T.; Kurashima, K. A novel precursor for synthesis of pure boron nitride nanotubes. *Chem. Commun.* **2002**, No. 12, 1290−1291.

(70) Tang, C. C.; Bando, Y.; Shen, G. Z.; Zhi, C. Y.; Golberg, D. Single-source precursor for chemical vapour deposition of collapsed boron nitride nanotubes. *Nanotechnology* **2006**, 17, 5882−5888.

(71) Terao, T.; Bando, Y.; Mitome, M.; Kurashima, K.; Zhi, C. Y.; Tang, C. C.; Golberg, D. Effective synthesis of surface-modified boron nitride nanotubes and related nanostructures and their hydrogen uptake. *Phys. E* **2008**, 40 (7), 2551−2555.

(72) Kim, J. H.; Pham, T. V.; Hwang, J. H.; Kim, C. S.; Kim, M. J. Dual growth mode of boron nitride nanotubes in high temperature pressure laser ablation. *Nano Converg* **2018**, 5, 17.

(73) Zhi, C.; Bando, Y.; Tan, C.; Golberg, D. Chemically activated boron nitride nanotubes. *Solid State Commun.* **2005**, 135, 67−70.

(74) Tang, C.; Bando, Y.; Sato, T.; Kurashima, K. nanotubes, A novel precursor for synthesis of pure boron nitride. *Chem. Commun.* **2002**, 1290−1291.

(75) Zhi, C.; Bando, Y.; Tan, C.; Golberg, D. Effective precursor for high yield synthesis of pure. *Solid State Commun.* **2005**, 135 (1-2), 67−70.

(76) Huang, Y.; Lin, J.; Tang, C.; Bando, Y.; Zhi, C.; Zhai, T.; Dierre, B.; Sekiguchi, T.; Golberg, D.; et al. Bulk synthesis,growth mechanism and properties of highly pure ultrafine boron nitride

nanotubes with diameters of sub-10 nm. *Nanotechnology* **2011**, *22*, 145602.

(77) Zhi, C.; Bando, Y.; Tang, C.; Golberg, D. Boron nitride nanotubes. *Mater. Sci. Eng. R* **2010**, *70* (3-6), 92−111.

(78) Lee, C. H.; Wang, J.; Kayatsha, V. K; Huang, J. Y; Yap, Y. K.; et al. Effective growth of boron nitride nanotubes by thermal chemical vapor deposition. *Nanotechnology* **2008**, *19*, 455605.

(79) Lee, C. H.; Xie, M.; Kayastha, V.; Wang, J.; Yap, Y. K. Patterned growth of boron nitride nanotubes by catalytic chemical vapor deposition. *Chem. Mater.* **2010**, *22* (5), 1782−1787, DOI: 10.1021/cm903287u.

(80) Boinovich, L. B.; Emelyanenko, A. M.; Pashinin, A. S.; Lee, C. H.; Drelich, J.; Yap, Y. K. Origins of Thermodynamically Stable Superhydrophobicity of Boron Nitride Nanotubes Coatings. *Langmuir* **2012**, *28* (2), 1206−1216, DOI: 10.1021/la204429z.

(81) Pakdel, A.; Zhi, C.; Bando, Y.; Nakayama, T.; Golberg, D.; et al. A comprehensive analysis of the CVD growth of boron nitride nanotubes. *Nanotechnology* **2012**, *23*, 215601.

(82) Lee, C. H.; Drelich, J.; Yap, Y. K. Superhydrophobicity of boron nitride nanotubes grown on silicon substrates. *Langmuir* **2009**, *25* (9), 4853−4860, DOI: 10.1021/la900511z.

(83) Chen, Y.; et al. A solid-state process for formation of boron nitride nanotubes. *Appl. Phys. Lett.* **1999**, *74*, 2960−2962.

(84) Li, L. H.; Chen, Y.; Glushenkov, A. M. Synthesis of boron nitride nanotubes by boron ink annealing. *Nanotechnology* **2010**, *21*, 105601.

(85) Li, L.; Liu, X.; Li, L.; Chen, Y. High yield BNNTs synthesis by promotion effect of milling-assisted precursor. *Microelectron. Eng.* **2013**, *110*, 256−259, DOI: 10.1016/j.mee.2013.01.044.

(86) Li, L. H.; Chen, Y.; Glushenkov. A.M. Boron nitride nanotube films grown from boron ink painting. *J. Mater. Chem.* **2010**, *20*, 9679−9683.

(87) Li, L.; Li, L. H.; Chen, Y.; Dai, X. J; Xing, T.; Petravic, M.; Liu, X. Mechanically activated catalyst mixing for high-yield boron nitride nanotube growth. *Nanoscale Res. Lett.* **2012**, *7*, 417.

(88) Arenal, R.; et al. A. Root-growth mechanism for single-walled boron nitride nanotubes in laser vaporization technique. *J. Am. Chem. Soc.* **2007**, *129*, 16183−16189.

(89) Lee, R. S.; Gavillet, J.; Chapelle, M. L. d. l.; Loiseau, A.; Cochon, J.-L.; Pigache, D.; Thibault, J.; Willaime, F.; et al. Catalyst-free synthesis of boron nitride single-wall nanotubes with a preferred zig-zag configuration. *Phys. Rev. B* **2001**, *64*, 64.

(90) Laude, T.; et al. Long ropes of boron nitride nanotubes grown by a continuous laser heating. *Appl. Phys. Lett.* **2000**, *76*, 3239−3241.

(91) Zhou, G. W.; Zhang, Z.; Bai, Z. G. Catalyst effects on formation of boron nitride nano-tubules synthesized by laser ablation. *Solid State Commun.* **1999**, *109* (8), 555−559.

(92) Wang, J.; et al. Low temperature growth of boron nitride nanotubes on substrates. *Nano Lett.* **2005**, *5*, 2528−2532.

(93) Smith, M. W; Jordan, K. C; Park, C.; Kim, J.-W.; Lillehei, P. T; Crooks, R.; Harrison, J. S; et al. Very long single-and few-walled boron nitride nanotubes via the pressurized vapor/condenser method. *Nanotechnology* **2009**, *20*, 505604.

(94) Smith, M. W; Jordan, K. C; Park, C.; Kim, J.-W.; Lillehei, P. T; Crooks, R.; Harrison, J. S; et al. Very long single-and few-walled boron nitride nanotubes via the pressurized vapor/condenser method. *Nanotechnology* **2009**, *20*, 505604.

(95) Tiano, A. L., et al.*Proc. SPIE 9060, Nanosensors, Biosensors, and Info-Tech Sensors and Systems*;Varadan, V. K., Ed.; SPIE: San Diego, CA, 2014; p 9060.

(96) Kim, K. S.; Kingston, C. T.; Hrdina, A.; Jakubinek, M. B.; Guan, J.; Plunkett, M.; Simard, B. Hydrogen-Catalyzed, Pilot-Scale Production of Small-Diameter Boron Nitride Nanotubes and Their Macroscopic Assemblies. *ACS Nano* **2014**, *8* (6), 6211−6220.

(97) Fathalizadeh, A.; et al. A. Scaled Synthesis of Boron Nitride Nanotubes, Nanoribbons, and Nanococoons Using Direct Feedstock Injection into an Extended-Pressure. *Inductively-Coupled Thermal Plasma Nano Lett.* **2014**, *14*, 4881−4886.

(98) Corso, M.; Auwarter, W.; Muntwiler, M.; Tamai, A.; Greber, T.; Osterwalder, J. Boron Nitride Nanomesh. *Science* **2004**, *303*, 217−220.

(99) Meziani, M. J.; Sheriff, K.; Parajuli, P.; Preigo, P.; Bhattacharya, S.; Rao, A. M.; Quimby, J. L.; Qiao, R.; Wang, P. Advances in Studies of Boron Nitride Nanosheets and Nanocomposites for Thermal Transport and Related Applications. *Chem. Eur.* **2022**, *23* (1), No. e202100645.

(100) Pacile, D.; Meyer, J. C.; Girit, C. O.; Zettl, A. The two-dimensional phase of boron nitride: Few-atomic-layer sheets and suspended membranes. *Appl. Phys. Lett.* **2008**, *92*, No. 133107.

(101) Meyer, J. C.; Chuvilin, A.; Algara-Siller, G.; Biskupek, J.; Kaiser, U. Selective Sputtering and Atomic Resolution Imaging of Atomically Thin Boron Nitride Membranes. *Nano Lett.* **2009**, *9*, 2683−2689.

(102) Gorbachev, R. V.; Riaz, I.; Nair, R. R.; Jalil, R.; Britnell, L.; Belle, B. D.; Hill, E. W.; Novoselov, K. S.; Watanabe, K.; Taniguchi, T.; Geim, A. K.; Blake, P. Hunting for monolayer boron nitride: optical and Raman signatures. *Small* **2011**, *7*, 465−468.

(103) Coleman, J. N.; Lotya, M.; O'Neill, A.; Bergin, S. D.; King, P. J.; Khan, U.; Young, K.; Gaucher, A.; De, S.; Smith, R. J.; Shvets, I. V.; Arora, S. K.; Stanton, G.; Kim, H.-Y.; Lee, K.; Kim, G. T.; Duesberg, G. S.; Hallam, T.; Boland, J. J.; Wang, J. J.; Donegan, J. F.; Grunlan, J. C.; Moriarty, G.; Shmeliov, A.; Nicholls, R. J.; Perkins, J. M.; Grieveson, E. M.; Theuwissen, K.; McComb, D. W.; Nellist, P. D.; Nicolosi, V. Two-dimensional nanosheets produced by liquid exfoliation of layered materials. *Science* **2011**, *331*, 568−571.

(104) Li, X.; Hao, X.; Zhao, M.; Wu, Y.; Yang, J.; Tian, Y.; Qian, G. Exfoliation of hexagonal boron nitride by molten hydroxides. *Adv. Mater.* **2013**, *25* (15), 2200−2204.

(105) Meyer, J. C.; Chuvilin, A.; Algara-Siller, G.; Biskupek, J.; Kaiser, U. Selective Sputtering and Atomic Resolution Imaging of Atomically Thin Boron Nitride Membranes. *Nano Lett.* **2009**, *9*, 2683−2689.

(106) Gorbachev, R. V.; Riaz, I.; Nair, R. R.; Jalil, R.; Britnell, L.; Belle, B. D.; Hill, E. W.; Novoselov, K. S.; Watanabe, K.; Taniguchi, T.; Geim, A. K.; Blake, P. Hunting for Monolayer Boron Nitride: Optical and Raman Signatures. *Small* **2011**, *7*, 465−468.

(107) Pacile, D.; Meyer, J. C.; Girit, Ç. O.; Zettl, A. The two-dimensional phase of boron nitride: Few-atomic-layer sheets and suspended membranes. *Appl. Phys. Lett.* **2008**, *92*, No. 133107.

(108) Deepika, L. H. Li.; Glushenkov, A. M.; Hait, S. K.; Hodgson, P.; Chen, Y. High-efficient production of boron nitride nanosheets via an optimized ball milling process for lubrication in oil. *Sci. Rep.* **2014**, *4*, 7288.

(109) Lei, W.; Mochalin, V. N.; Liu, D.; Qin, S.; Gogotsi, Y.; Chen, Y. Boron nitride colloidal solutions, ultralight aerogels and free-standing membranes through one-step exfoliation and functionalization. *Nat. Commun.* **2015**, *6*, 8849.

(110) Wang, Z. D.; Meziani, M. J.; Patel, A. K.; Priego, P.; Wirth, W.; Wang, P.; Sun, Y.-P. Dispersion of high-quality boron nitride nanosheets in polyethylene for nanocomposites of superior thermal transport properties. *Ind. Eng. Chem. Res.* **2019**, *58*, 18644−18653.

(111) Griffin, A.; Harvey, A.; Cunningham, B.; Scullion, D.; Tian, T.; Shih, C.-J.; Gruening, M.; Donegan, J. F; Santos, E. J. G.; Backes, C.; Coleman, J. N. Spectroscopic size and thickness metrics for liquid-exfoliated h-BN. *Chem. Mater.* **2018**, *30* (6), 1998.

(112) Anderson, A.; Hou, Z.-L.; Song, W.-L.; Meziani, M. J.; Wang, P.; Lu, F.; Lee, J.; Xu, L.; Sun, Y.-P. Towards nanostructured boron nitride films. *Mater. Sci. Mater. Electron* **2017**, *28*, 9048−9055.

(113) Sun, W.; Meng, Y.; Fu, Q.; Wang, F.; Wang, G.; Gao, W.; Huang, X.; Lu, F. High-Yield Production of Boron Nitride Nanosheets and Its Uses as a Catalyst Support for Hydrogenation of Nitroaromatics. *ACS Appl. Mater. Interfaces* **2016**, *8*, 9881−9888.

(114) Yang, F.; Sun, X.; Yao, Z. Thionyl Chloride Corrodes Hexagonal Boron Nitride to Generate. *Langmuir* **2021**, *37*, 6442−6450.

(115) Guo, Y.; Ruan, K.; Shi, X.; Yang, X.; Gu, J. Factors affecting thermal conductivities of the polymers and polymer composites: A review. *Compos. Sci. Technol.* 2020, 193, 108134.

(116) Yan, Q.; Dai, W.; Gao, J.; Tan, X.; Lv, L.; Ying, J.; Lu, X.; Lu, J.; Yao, Y.; Wei, Q.; Sun, R.; Yu, J.; Jiang, N.; Chen, D.; Wong, C.-P.; Xiang, R.; Maruyama, S.; Lin, C.-T. Soft and Self-Adhesive Thermal Interface Ultrahigh-Aspect-Ratio Boron Nitride Nanosheets Leading to Superhigh In-Plane Thermal Conductivity of Foldable Heat. *ACS Nano* 2021, 15, 6489−6498.

(117) Ma, J.; Luo, N.; Xie, Z.; Chen, F.; Fu, Q. Preparation of modified hexagonal boron nitride by ball-milling and enhanced thermal conductivity of epoxy resin. *Materi. Res. Express* 2019, 6, 1050d8.

(118) Shaocheng Li; Xianlang Lu; Yanda Lou; Kejun Liu; Benxue Zou. The Synthesis and Characterization of h-BN Nanosheets with High. *ACS Omega* 2021, 6 (42), 27814−27822.

(119) Han, W. Q.; Wu, L.; Zhu, Y.; Watanabe, K.; Taniguchi, T. Structure of chemically derived mono- and few-atomic-layer boron nitride sheets. *Appl. Phys. Lett.* 2008, 93, 223103 DOI: 10.1063/1.3041639.

(120) Lin, Y.; Williams, T. V.; Connell, J. W. Soluble, Exfoliated Hexagonal Boron Nitride Nanosheets. *J. Phys. Chem. C* 2010, 1, 277−283.

(121) Smith, R. J.; King, P. J.; Lotya, M.; Wirtz, C.; Khan, U.; De, S.; O'Neill, A.; Duesberg, G. S.; Grunlan, J. C.; Moriarty, G.; Chen, J. Large-Scale Exfoliation of Inorganic Layered Compounds in Aqueous Surfactant Solutions. *Adv. Mater.* 2011, 23 (34), 3944−3948, DOI: 10.1002/adma.201102584.

(122) Wang, Y.; Shi, Z.; Yin, J. Boron nitridenanosheets: large-scale exfoliation in methanesulfonic acid and their composites with polybenzimidazole. *J. Mater. Chem.* 2011, 21, 11371−11377.

(123) Coleman, J. N.; Lotya, M.; O'Neill, A.; Bergin, S. D.; King, P. J.; Khan, U.; Young, K.; Gaucher, A.; De, S.; Smith, R. J.; Shvets, I. V.; Arora, S. K.; Stanton, G.; Kim, H.-Y.; Lee, K.; Kim, G. T.; Duesberg, G. S.; Hallam, T.; Boland, J. J.; Wang, J. J.; Donegan, J. F.; Grunlan, J. C.; Moriarty, G.; Shmeliov, A.; Nicholls, R. J.; Perkins, J. M.; Grieveson, E. M.; Theuwissen, K.; McComb, D. W.; Nellist, P. D.; Nicolosi, V. Two-dimensional nanosheets produced by liquid exfoliation of layered materials. *Science* 2011, 331, 568.

(124) Tao, H.; Zhang, Y.; Gao, Y.; Sun, Z.; Yan, C.; Texter, J. Scalable exfoliation and dispersion of two-dimensional materials — an update. *Phys. Chem. Chem. Phys.* 2017, 19, 921−960.

(125) Coleman, J. N.; Lotya, M.; O'Neill, A.; Bergin, S. D.; King, P. J.; Khan, U.; Young, K.; Gaucher, A.; De, S.; Smith, R. J.; Shvets, I. V.; Arora, S. K.; Stanton, G.; Kim, H.-Y.; Lee, K.; Kim, G. T.; Duesberg, G. S.; Hallam, T.; Boland, J. J.; Wang, J. J.; Donegan, J. F.; Grunlan, J. C.; Moriarty, G.; Shmeliov, A.; Nicholls, R. J.; Perkins, J. M.; Grieveson, E. M.; Theuwissen, K.; McComb, D. W.; Nellist, P. D.; Nicolosi, V. Two-Dimensional Nanosheets Produced by Liquid Exfoliation of Layered Materials. *Science* 2011, 331, 568−571.

(126) Camilli, L.; Sutter, E.; Sutter, P. Growth of two-dimensional materials on non-catalytic substrates: h-BN/Au(111). *2D Mater.* 2005, 1 (2), 3464−3467.

(127) Auwarter, W.; Suter, H. U.; Sachdev, H.; Greber, T. Synthesis of One Monolayer of Hexagonal Boron Nitride on Ni(111) from B-Trichloroborazine (ClBNH)3. *Chem. Mater.* 2004, 16, 343−345.

(128) Hyun, W. J.; de Moraes, A. C. M.; Lim, J.-M.; Downing, J. R.; Park, K.-Y.; Tan, M. T. Z.; Hersam, M. C. High-Modulus Hexagonal Boron Nitride Nanoplatelet Gel Electrolytes for Solid-State Rechargeable Lithium-Ion Batteries. *Adv. Funct. Mater.* 2019, 13, No. 9664.

(129) Ge, X.; Liang, W. J.; Ge, J. F.; Chen, X. J.; Ji, J. Y.; Pang, X. Y.; He, M.; M Feng, X. Hexagonal Boron Nitride/Microfibril Cellulose/Poly(vinyl alcohol) Ternary Composite Film with Thermal Conductivity and Flexibility. *Mater.* 2019, 12 (1), 104.

(130) Muhabie, A. A.; Cheng, C.-C.; Huang, J.-J.; Liao, Z.-S.; Huang, S.-Y.; Chiu, C.-W.; Lee, D.-J. Non-Covalently Functionalized Boron Nitride Mediated by a Highly Self-Assembled Supramolecular Polymer. *Chem. Mater.* 2017, 29 (19), 8513−8520.

(131) Wang, Z.; Wen, Y.; Zhao, S.; Zhang, W.; Ji, Y.; Zhang, S.; Li, J. Molybdenum oxynitride nanoparticles on nitrogen-doped CNT architectures for the oxygen evolution reaction. *Ind. Crops Prods.* 2019, 137, 239−247.

(132) Paffett, M. T.; Simonson, R. J.; Papin, P.; Paine, R. T. Borazine adsorption and decomposition at Pt(111) and Ru(001) surfaces. *Surf. Sci.* 1990, 232 (3), 286−296.

(133) Ismach, A.; Chou, H.; Ferrer, D. A.; Wu, Y.; McDonnell, S.; Floresca, H. C.; Covacevich, A.; Pope, C.; Piner, R.; Kim, M. J.; Wallace, R. M.; Colombo, L.; Ruoff, R. S. Toward the controlled synthesis of hexagonal boron nitride films. *ACS Nano* 2012, 6 (7), 6378−6385.

(134) Tay, R. Y.; Li, H.; Tsang, S. H.; Zhu, M.; Loeblein, M.; Jing, L.; Leong, F. N.; Teo, E. H. T. Composition-controlled synthesis and tunable optical properties of ternary boron carbonitride nanotubes. *Chem. Mater.* 2016, 28, 2180−2190.

(135) Park, J. H.; Choi, S. H.; Zhao, J.; Song, S.; Yang, W.; Kim, S. M.; Kim, K. K.; Lee, Y. H. Low-Threshold Nanolasers Based on Slab-Nanocrystals of H-Aggregated Organic Semiconductors. *Curr. Appl. Phys.* 2016, 16, 1229−1235.

(136) Park, J.-H.; Park, J. C.; Yun, S. J.; Kim, H.; Luong, D. H.; Kim, S. M.; Choi, S. H.; Yang, W.; Kong, J.; Kim, K. K.; Lee, Y. H. Large-Area Monolayer Hexagonal Boron Nitride on Pt Foil. *ACS Nano* 2014, 8 (8), 8520−8528.

(137) Lee, Y. H.; Liu, K. K.; Lu, A. Y.; Wu, C. Y.; Lin, C. T.; Zhang, W.; Su, C. Y.; Hsu, C. L.; Lin, T. W.; Wei, K. H.; Shi, Y.; Li, L. J. Growth selectivity of hexagonal-boron nitride layers on Ni with various crystal orientations. *RSC Adv.* 2012, 2, 111−115.

(138) Shi, Y.; Hamsen, C.; Jia, X.; Kim, K. K.; Reina, A.; Hofmann, M.; Hsu, A. L.; Zhang, K.; Li, H.; Juang, Z.-Y.; Dresselhaus, M. S.; Li, L.-J.; Kong, J. Synthesis of few-layer hexagonal boron nitride thin film by chemical vapor deposition. *Nano Lett.* 2010, 10 (10), 4134−4139.

(139) Charlier, J.-C.; Blase, X.; Roche, S. Electronic and transport properties of nanotubes. *Rev. Mod. Phys.* 2007, 79, 677.

(140) Zhi, C.; Bando, Y.; Terao, T.; Tang, C. C.; Kuwahara, H.; Golberg, D. Chemically activated boron nitride nanotubes. *Chem. Asian J.* 2009, 4, 1536−40.

(141) Lauret, J. S.; Arenal, R.; Ducastelle, F.; Loiseau, A.; Cau, M.; Attal-Tretout, B.; Rosencher, E.; Goux-Capes, L. Optical transitions in single-wall boron nitride nanotubes. *Phys. Rev. Lett.* 2005, 94, 037405.

(142) Jaffrennou, P.; Barjon, J.; Schmid, T.; Museur, L.; Kanaev, A.; Lauret, J.; Zhi, C.; Tang, C.; Bando, Y.; Golberg, D.; Attal-Tretout, B.; Ducastelle, F.; Loiseau, A. Near-band-edge recombinations in multiwalled boron nitride nanotubes: Cathodoluminescence and photoluminescence spectroscopy measurements. *Phys. Rev. B* 2008, 77, 235422.

(143) Nasrabadi, A. T.; Foroutan, M. Interactions between polymers and single-walled boron nitride nanotubes: a molecular dynamics simulation approach. *J. Phys. Chem. B* 2010, 114, 15429−15436.

(144) Zeng, H. B.; Zhi, C. Y.; Zhang, Z. H.; Wei, X. L.; Wang, X. B.; Guo, W. L.; Bando, Y.; Golberg, D. "White graphenes": boron nitride nanoribbons via boron nitride nanotube unwrapping. *Nano Lett.* 2010, 10 (12), 5049−5055.

(145) Peralta, V.; Barone. *Magnetic boron nitride nanoribbons with tunable electronic properties Nano Lett.* 2008, 8, 2210−2214.

(146) Zhi, C. Y.; Hanagata, N.; Bando, Y.; Golberg, D. Dispersible Shortened Boron Nitride Nanotubes with Improved Molecule-Loading Capacity. *Chem.-Asian J.* 2011, 6, 2530−2535.

(147) Chen, Y.; Zou, J.; Campbell, S. J.; Le Caer, G. Boron nitride nanotubes: Pronounced resistance to oxidation. *Appl. Phys. Lett.* 2004, 84, 2430−2432.

(148) Zhi, C. Y.; Bando, Y.; Tang, C. C.; Huang, Q.; Golberg, D. Chemically activated boron nitride nanotubes. *Chem. Asian J.* 2008, 4 (10), 1536−1540.

(149) Liu, Z.; Gong, Y. J.; Zhou, W.; Ma, L. L.; Yu, J. J.; Idrobo, J. C.; Jung, J.; MacDonald, A. H.; Vajtai, R.; Lou, J.; Ajayan, P. M. Ultrathin high-temperature oxidation-resistant coatings of hexagonal boron nitride. *Nat. Commun.* 2013, 4, 2541.

(150) Li, L. H.; Cervenka, J.; Watanabe, K.; Taniguchi, T.; Chen, Y. Strong oxidation resistance of atomically thin boron nitride nanosheets. *ACS Nano* **2014**, *8* (2), 1457−1462.

(151) Xu, Z.; Golberg, D.; Bando, Y. Boron nitride nanotubes and nanosheets. *Nano Lett.* **2009**, *9*, 2251−2254.

(152) Chang, C. W.; Okawa, D.; Garcia, H.; Majumdar, A. Breakdown of Fourier's law in nanotube thermal conductors. *Phys. Rev. Lett.* **2008**, *101*, 903.

(153) Berber, S.; Kwon, Y. K.; Tomanek, D. Unusually High Thermal Conductivity of Carbon Nanotubes. *Phys. Rev. Lett.* **2000**, *84*, 4613.

(154) Xiao, Y.; Yan, X. H.; Cao, J. X.; Ding, J. W.; Mao, Y. L.; Xiang, J. Specific heat and quantized thermal conductance of single-walled boron nitride nanotubes. *Phys. Rev. B* **2004**, *69*, 205415.

(155) Zettl, A.; Chang, C. W.; Begtrup, G. A new look at thermal properties of nanotubes. *Phys. Stat. Solidi B* **2007**, *244* (11), 4181−4183.

(156) Chang, C. W.; Fennimore, A. M.; Afanasiev, A.; Okawa, D.; Ikuno, T.; Garcia, H.; Li, D. Y.; Majumdar, A.; Zettl, A. Isotope Effect on the Thermal Conductivity of Boron Nitride Nanotubes. *Phys. Rev. Lett.* **2006**, *97*, 085901.

(157) Chang, C. W.; Han, W. Q.; Zettl, A. Thermal conductivity of B−C−N and BN nanotubes. *Appl. Phys. Lett.* **2005**, *86*, No. 173102.

(158) Chang, C. W.; Han, W. Q.; Zettl, A.*J. Vac. Sci. Technol., B* **2009**, 199.

(159) Tang, C. C.; Bando, Y.; Liu, B. D.; Golberg, D. Cerium Oxide Nanotubes Prepared from Cerium Hydroxide Nanotubes. *Adv. Mater.* **2005**, *17* (24), 3005−3009.

(160) Li, B.; Yang, B.; Yuan, J. Stable block copolymer single material organic solar cells: progress and perspective. *Energy Environ. Sci.* **2023**, *16*, 723−744.

(161) Tao, O. Y.; Chen, Y. P.; Xie, Y. E.; Yang, K. K.; Bao, Z. G.; Zhong, J. X. Thermal transport in hexagonal boron nitride nanoribbons. *Nanotechnol.* **2010**, *21* (24), 245701.

(162) Lindsay, L.; Broido, D. A. Enhanced thermal conductivity and isotope effect in single-layer hexagonal boron nitride. *Phys. Rev. B* **2011**, *84*, No. 155421.

(163) Lindsay, L.; Broido, D. A. Theory of thermal transport in multilayer hexagonal boron nitride and nanotubes. *Phys. Rev. B* **2012**, *85*, No. 035436.

(164) Zettl; Chopra, N. G. Measurement of the elastic modulus of a multi-wall boron nitride nanotube. *Solid State Commun.* **1998**, *105*, 297−300.

(165) Hernandez, E.; Goze, C.; Bernier, P.; Rubio, A. Elastic properties of single-wall nanotubes. *Appl. Phys. A: Mater. Sci. Process.* **1999**, *68*, 287−292.

(166) Peng, Y. J.; Zhang, L. Y.; Jin, Q. H.; Li, B. H.; Ding, D. T. Ab initio studies of elastic properties and electronic structures of C and BN nanotubes. *Phys. E* **2006**, *33*, 155−159.

(167) Verma, V.; Jindal, V. K.; Dharamvir, K. Elastic moduli of a boron nitride nanotube. *Nanotechnology* **2007**, *18*, No. 435711.

(168) Dumitrica, T.; Bettinger, H. F.; Scuseria, G. E.; Yakobson, B. I. Thermodynamics of yield in boron nitride nanotubes. *Phys. Rev. B* **2003**, *68*, No. 085412.

(169) Boldrin, L.; Scarpa, F.; Chowdhury, R.; Adhikari, S. Effective mechanical properties of hexagonal boron nitride nanosheets. *Nanotechnology* **2011**, *22*, No. 505702.

(170) Yuan, J. H.; Liew, K. M. High-Temperature Thermal Stability and In-Plane Compressive Properties of a Graphene and Boron-Nitride Nanosheet. *J. Nanosci. Nanotechnol* **2012**, *12*, 2617−2624.

(171) Peng, Q.; Ji, W.; De, S. Mechanical properties of the hexagonal boron nitride monolayer: Ab initio study. *Comput. Mater. Sci.* **2012**, *56*, 11−17.

(172) Zhi, C. Y.; Bando, Y.; Tang, C. C.; Xie, R. G.; Sekiguchi, T.; Golberg, D. Perfectly dissolved boron nitride nanotubes due to polymer wrapping. *J. Am. Chem. Soc.* **2005**, *127*, 15996−15997.

(173) Lin, Y.; Williams, T. V.; Connell, J. W. Soluble, Exfoliated Hexagonal Boron Nitride Nanosheets. *J. Phys. Chem. Lett.* **2010**, *1*, 277−283.

(174) Gao, R.; Yin, L. W.; Wang, C. X.; Qi, Y. X.; Lun, N.; Zhang, L. Y.; Liu, Y. X.; Kang, L.; Wang, X. F. Boron Nitride Nanosheets: novel Syntheses and Applications in polymeric Composites. *J. Phys. Chem. C* **2009**, *113*, 15160−15165.

(175) Hua Li, L.; Chen, Y.; Cheng, B.-M.; Lin, M.-Y.; Chou, S.-L.; Peng, Y.-C. Evidence for Dirac Fermions in a Honeycomb Lattice Based on Silicon. *Appl. Phys. Lett.* **2012**, *100*, No. 261108.

(176) Pakdel, A.; Wang, X. B.; Zhi, C. Y.; Bando, Y.; Watanabe, K.; Sekiguchi, T.; Nakayama, T.; Golberg, D. Large-surface-area BN nanosheets and their utilization in polymeric composites with improved thermal and dielectric properties. *J. Mater. Chem.* **2012**, *22*, 4818−4824.

(177) Zhao, Z. Y.; Yang, Z. G.; Wen, Y.; Wang, Y. H. Structural Sensitivities in Bimetallic Catalysts for Electrochemical CO2 Reduction Revealed by Ag−Cu Nanodimers. *J. Am. Ceram. Soc.* **2011**, *94*, 4496−4501.

(178) Liu, S.; Ji, J.; Zeng, H.; Xie, Z.; Song, X.; Zhou, S.; Chen, P. Functionalization of hexagonal boron nitride nanosheets and their copolymerized solid glasses. *2D Materials* **2018**, *5*, No. 035036.

(179) *Organisation, World Health. Radiation: Ultraviolet (UV) radiation.* World Health Organisation. https://www.who.int/news-room/questions-and-answers/item/radiation-ultraviolet-(uwebv; [Online] March 9, 2016. [Cited: 12−21−2021] .

(180) Marti; Gordillo, M. C. Wetting and prewetting of water on top of a single sheet of hexagonal boron nitride. *phys. Rev. E: Stat., Nonlinear Soft Matter Phys.* **2011**, *84*, No. 011602.

(181) Pakdel, A.; Bando, Y.; Golberg, D. Morphology-Driven Nonwettability of Nanostructured BN Surfaces. *Langmuir* **2013**, *29*, 7529−7533.

(182) Zeng; Li, H. Wetting and interfacial properties of water nanodroplets in contact with graphene and monolayer boron-nitride sheets. *ACS Nano* **2012**, *6*, 2401−2409.

(183) Zhang, S. J.; Lian, G.; Si, H. B.; Wang, J.; Zhang, X.; Wang, Q. L.; Cui, D. L. Ultrathin BN nanosheets with zigzag edge: one-step chemical synthesis, applications in wastewater treatment and preparation of highly thermal-conductive BN−polymer composites. *J. Mater. Chem. A* **2013**, *1*, 5105−5112.

(184) Muller, K.; Bugnicourt, E.; Latorre, M.; Jorda, M.; Echegoyen Sanz, Y.; Lagaron, J.; Miesbauer, O.; Bianchin, A.; Hankin, S.; Bolz, U.; Perez, G.; Jesdinszki, M.; Lindner, M.; Scheuerer, Z.; Castello, S.; Schmid, M. Review on the Processing and Properties of Polymer Nanocomposites and Nanocoatings and Their Applications in the Packaging, Automotive and Solar Energy Fields. *Nanomaterials* **2017**, *7*, 74.

(185) Tjong, S. C. Structural and mechanical properties of polymer nanocomposites. *Mater. Sci. Eng. R: Rep.* **2006**, *53*, 73−197.

(186) Biscarat, J.; Bechelany, M.; Pochat-Bohatier, C.; Miele, P. Graphene-like BN/gelatin nanobiocomposites for gas barrier applications. *NanoScale* **2015**, *7*, 613−618.

(187) Alva, G.; Lin, Y.; Fang, G. Thermal and electrical characterization of polymer/ceramic composites with polyvinyl butyral matrix. *Mater. Chem. Phys.* **2018**, *205*, 401−415.

(188) Dantas de Oliveira, A.; Augusto Goncalves Beatrice, C.Polymer nano composites with different types of nanofiller*Nano-composites - Recent Evolutions*; InTech Open, 2019 DOI: 10.5772/intechopen.81329.

(189) Uysal Unalan, I.; Cerri, G.; Marcuzzo, E.; Cozzolino, C. A.; Farris, S. Nanocomposite films and coatings using inorganic nanobuilding blocks (NBB): current applications and future opportunities in the food packaging sector. *RSC Adv.* **2014**, *4*, 29393−29428.

(190) Wang, Z.; Li, Q.; Chen, Z.; Liu, J.; Liu, T.; Li, H.; Zheng, S. Enhanced comprehensive properties of nylon-6 nanocomposites by aniline-modified boron nitride nanosheets. *Ind. Eng. Chem. Res.* **2018**, *57*, 11005−11013.

(191) Liu, Y.; Goebl, J.; Yin, Y. Templated synthesis of nano-structured materials. *Chem. Soc. Rev.* **2013**, *42*, 2610−2653, DOI: 10.1039/C2CS35369E.

(192) Zeng, X.; Yao, Y.; Gong, Z.; Wang, F.; Sun, R.; Xu, J.; Wong, C. P. Ice templated assembly strategy to construct 3D boron nitride nanosheet networks in polymer composites for thermal conductivity improvement. *Small* 2015, 11, 6205−6213.

(193) Gonzalez Ortiz, D.; Pochat-Bohatier, C.; Cambedouzou, J.; Bechelany, M.; Miele, P. Current trends in pickering emulsions: particle morphology and applications. *Eng.* 2020, 6 (4), 468−482, DOI: 10.1016/j.eng.2019.08.017.

(194) Nayak, R. K.; Mahato, K. K.; Ray, B. C.Processing of polymer-based nanocomposites*Reinforced Polymer Composites: Processing, Characterization and Post Life Cycle Assessment*; Wiley; New York, 2019; pp 55−75 DOI: 10.1002/9783527820979.ch4.

(195) Song, W.-L.; Wang, P.; Cao, L.; Anderson, A.; Meziani, M. J.; Farr, A. J.; Sun, Y.-P. Polymer/boron nitride nanocomposite materials for superior thermal transport performance. *Angew. Chem. Int. Ed.* 2012, 51, 6498−6501.

(196) Morishita, T.; Okamoto, H. Facile exfoliation and noncovalent superacid functionalization of boron nitride nanosheets and their use for highly thermally conductive and electrically insulating polymer nanocomposites. *ACS Appl. Mater. Interfaces* 2016, 8, 27064−27073.

(197) Zhang, X.; Chen, H.; Ye, H.; Liu, A.; Xu, L. Enhanced interfacial polarization in poly(vinylidene fluoride- chlorotrifluoro-ethylene) nanocomposite with parallel boron nitride nanosheets. *Nanotechnology* 2020, 31, No. 165703.

(198) Xie, S. Y.; Wang, W.; Fernando, K. A. S.; Wang, X.; Lin, Y.; Sun, Y. P. Quantum-sized carbon dots for bright and colorful photoluminescence. *JACS* 2005, 128 (24), 3670−3672, DOI: 10.1021/ja062677d.

(199) Zhi, C. Y.; Zhang, L. J.; Bando, Y.; Terao, T.; Tang, C. C.; Kuwahara, H.; Golberg, D. Boron nitride nanotubes: functionalization and composites. *J. Phys. Chem. C* 2008, 112, 17592−17595.

(200) Zhi, C. Y.; Bando, Y.; Tang, C. C.; Honda, S.; Sato, K.; Kuwahara, H.; Golberg, D. *Covalent functionalization: towards soluble multiwalled boron nitride nanotubes Angew. Chem.* 2005, 44, 7929−7932.

(201) Velayudham, S.; Lee, C. H.; Xie, M.; Blair, D.; Bauman, N.; Yap, Y. K.; Green, S. A.; Liu, H. Noncovalent functionalization of boron nitride nanotubes with poly(p-phenylene-ethynylene)s and polythiophene. *ACS Appl. Mater. Interfaces* 2010, 2, 104−110.

(202) Liu, F.; Mo, X. S.; Gan, H. B.; Guo, T. Y.; Wang, X. B.; Chen, B.; Chen, J.; Deng, S. Z.; Xu, N. S.; Sekiguchi, T.; Golberg, D.; Bando, Y. Cheap, Gram-Scale Fabrication of BN Nanosheets via Substitution Reaction of Graphite Powders and Their Use for Mechanical Reinforcement of Polymers. *Sci. Rep.* 2014, 4, 4211.

(203) Wang, X. B.; Pakdel, A.; Zhi, C. Y.; Watanabe, K.; Sekiguchi, T.; Golberg, D.; Bando, Y. High-yield boron nitride nanosheets from 'chemical blowing': towards practical applications in polymer composites. *J. Phys.: Condens. Matter* 2012, 24, No. 314205.

(204) Jan, R.; May, P.; Bell, A. P.; Habib, A.; Khan, U.; COleman, J. N. Enhancing the mechanical properties of BN nanosheet−polymer composites by uniaxial drawing. *Nanoscale* 2014, 6, 4889−4895.

(205) Terao, T.; Bando, Y.; Mitome, M.; Zhi, C. Y.; Tang, C. C.; Golberg, D. Thermal conductivity improvement of polymer films by catechin-modified boron nitride nanotubes. *J. Phys. Chem. C* 2009, 113, 13605−13609.

(206) Wu, K.; Fang, J.; Ma, J.; Huang, R.; Chai, S.; Chen, F.; Fu, Q. Achieving a Collapsible, Strong, and Highly Thermally Conductive Film Based on Oriented Functionalized Boron Nitride Nanosheets and Cellulose Nanofiber. *ACS Appl. Mater. Interfaces* 2017, 9, 30035−30045.

(207) Chung; Xu, Y. S. Increasing the thermal conductivity of boron nitride and aluminum nitride particle epoxy-matrix composites by particle surface treatments. *Compos. Interfaces* 2000, 7, 243−256.

(208) Wattanakul, K.; Manuspiya, H.; Yanumet, N. Effective surface treatments for enhancing the thermal conductivity of BN-filled epoxy composite. *j. Appl. Polym.sci.* 2011, 119, 3234−3243.

(209) Yu, J. H.; Huang, X. Y.; Wu, C.; Wu, X. F.; Wang, G. L.; Jiang, P. K. Interfacial modification of boron nitride nanoplatelets for epoxy composites with improved thermal properties. *Polymer* 2012, 53 (2), 471−480, DOI: 10.1016/j.polymer.2011.12.040.

(210) Huang, X. Y.; Zhi, C. Y.; Jiang, P. K.; Golberg, D.; Bando, Y.; Tanaka, T. Mechanically Flexible and Multifunctional Polymer-Based Graphene Foams for Elastic Conductors and Oil-Water Separators. *Adv. Funct. Mater.* 2013, 23, 1824−1831.

(211) Cho, H. B.; Tu, N. C.; Fujihara, T.; Endo, S.; Suzuki, T.; Tanaka, S.; Jiang, W. H.; Suematsu, H.; Niihara, K.; Nakayama, T. Epoxy resin-based nanocomposite films with highly oriented BN nanosheets prepared using a nanosecond-pulse electric field. *Mater. Lett.* 2011, 65, 2426−2428.

(212) Cho, H. B.; Tokoi, Y.; Tanaka, S.; Suematsu, H.; Suzuki, T.; Jiang, W. H.; Niihara, K.; Nakayama, T. Modification of BN nanosheets and their thermal conducting properties in nanocomposite film with polysiloxane according to the orientation of BN. *Compos. Sci. Technol.* 2011, 71, 1046−1052.

(213) Cho, H. B.; Mitsuhashi, M.; Nakayama, T.; Tanaka, S.; Suzuki, T.; Suematsu, H.; Jiang, W. H.; Tokoi, Y.; Lee, S. W.; Park, Y. H.; Niihara, K. Thermal anisotropy of epoxy resin-based nano-hybrid films containing BN nanosheets under a rotating superconducting magnetic field. *Mater. Chem. Phys.* 2013, 139, 355−359.

(214) Lim, H. S.; Oh, J. W.; Kim, S. Y.; Yoo, M. J.; Park, S. D.; Lee, W. S. Colloidal Photonic Crystals toward Structural Color Palettes for Security Materials. *Chem. Mater.* 2013, 25, 3315−3319.

(215) Terao, T.; Zhi, C. Y.; Bando, Y.; Mitome, M.; Tang, C. C.; Golberg, D. Alignment of Boron Nitride Nanotubes in Polymeric Composite Films for Thermal Conductivity Improvement. *J. Phys. Chem. C* 2010, 114, 4340−4344.

(216) Meziani, M. J.; Song, W.-L.; Wang, P.; Lu, F.; Hou, Z.; Anderson, A.; Maimaiti, H.; Sun, Y.-P. Boron Nitride Nanomaterials for Thermal Management Applications. *ChemPhysChem* 2015, 16, 1339−1346.

(217) Wu, K.; Liao, P.; Du, R.; Zhang, Q.; Chen, F.; Fu, Q. Preparation of a thermally conductive biodegradable cellulose nanofiber/hydroxylated boron nitride nanosheet film: the critical role of edge-hydroxylation. *J. Mater. Chem. A* 2018, 6, 11863−11873.

(218) Morishita, T.; Okamoto, H. A high-yield ionic liquid-promoted synthesis of boron nitride nanosheets by direct exfoliation. *ACS Appl. Mater. Interfaces* 2016, 8, 27064−27073.

(219) Seo, T. H.; et al. Boron nitride nanotubes as a heat sinking and stress-relaxation layer for high performance light-emitting diodes. *Nanoscale* 2017, 9 (42), 16223−16231.

(220) Zhang, D.; Zhang, S.; Yapici, N.; Oakley, R.; Sharma, S.; Parashar, V.; Yap, Y. K. Emerging Applications of Boron Nitride Nanotubes in Energy Harvesting, Electronics, and Biomedicine. *ACS Omega* 2021, 6, 20722−20728.

(221) Lee, C. H.; et al. Room Temperature Tunneling Behavior of Boron Nitride Nanotubes Functionalized with Gold Quantum Dots. *Adv. Mater.* 2013, 25, 4544−4548.

(222) Hao, B.; Asthana, A.; Hazaveh, P. K.; Bergstrom, P. L.; Banyai, D.; Savaikar, M. A.; Jaszczak, J. A.; Yap, Y. K.; et al. New Flexible Channels for Room Temperature Tunneling Field Effect Transistors. *Scitific Reports* 2016, 6 (1), No. 20293.

(223) Qin, J.-K.; et al. Raman response and transport properties of tellurium atomic chains encapsulated in nanotubes. *Nature Electronics* 2020, 3, 141−147.

(224) Wang, J.; Zhang, L.; Wang, L.; Lei, W.; Wu, Z.-S. Two-dimensional Boron Nitride for Electronics and Energy Applications. *Energy Environ. Mater.* 2022, 5 (1), 10−44, DOI: 10.1002/eem2.12159.

(225) Gao, T.; Song, X.; Du, H.; Nie, Y.; Chen, Y.; Ji, Q.; Sun, J.; Yang, Y.; Zhang, Y.; Liu, Z. Temperature-triggered chemical switching growth of in-plane and vertically stacked graphene-boron nitride heterostructures. *Nat. Commun.* 2015, 6, 6835.

(226) Wang, L.; Wu, B.; Liu, H.; Wang, H.; Su, Y.; Lei, W.; Hu, P.; Liu, Y. An intrinsically stretchable humidity sensor based on anti-drying, self-healing and transparent organohydrogels. *Sci. material* 2019, 62, 1218.

(227) Lin, Z.; Mcnamara, A.; Liu, Y.; Moon, K.-s.; Wong, C.-P. Exfoliated hexagonal boron nitride-based polymer nanocomposite with enhanced thermal conductivity for electronic encapsulation. *Compos. Sci. Technol.* **2014**, *90*, 123−128.

(228) Zou, C.; Zhang, C.; Li, B.; Wang, S.; Xie, Z.; Song, Y. Fabrication and properties of borazine derived boron nitride matrix wave-transparent composites reinorced by 2.5 dimensional fabric of Si-N-O fibers. *Mater. Sci. Eng.* **2015**, *620*, 420−427.

(229) Zhang, J.; Wang, X.; Yu, C.; Li, Q.; Li, Z.; Li, C.; Lu, H.; Zhang, Q.; Zhao, J.; Hu, M.; Yao, Y. A facile method to prepare flexible boron nitride/poly(vinyl alcohol) composites with enhanced thermal conductivity. *Compos. Sci. Technol.* **2017**, *149*, 41−47.

(230) Meng, J. H.; Liu, X.; Zhang, X. W.; Zhang, Y.; Wang, H. L.; Yin, Z. G.; Zhang, Y. Z.; Liu, H.; You, J. B.; Yan, H. Interface engineering for highly efficient graphene-on-silicon Schottky junction solar cells by introducing a hexagonal boron nitride interlayer. *Nano Energy* **2016**, *28*, 44−50.

(231) Cho, A. J.; Kwon, J. Y. Hexagonal boron nitride for surface passivation of two dimensional van der Waals heterojunction solar cells. *ACS Appl. Mater. Interfaces* **2019**, *11*, 39765−39771.

(232) Green, M. A.; Ho-Baillie, A.; Snaith, H. J. The emergence of perovskite solar cells. *Nat. Photonics* **2014**, *8*, 506−514.

(233) Yang, S.; Fu, W.; Zhang, Z.; Chen, H.; Li, C. Z. Recent advances in perovskite solar cells: efficiency, stability and lead-free perovskite. *J. Mater. Chem.* **2017**, *5*, 11462−11482.

(234) Seitz, M.; Gant, P.; Castellanos-Gomez, A.; Prins, F. Long-term stabilization of two-dimensional perovskites by encapsulation with hexagonal boron. *Nanomaterials* **2019**, *9*, 1120.

(235) Zhang, H.; Tong, C. J.; Zhang, Y.; Zhang, Y. N.; Liu, L. M. *Porous BN for hydrogen generation and storage J. Mater. Chem.* **2015**, *3*, 9632−9637.

(236) Lim, S.H.; Luo, J.; Ji, W.; Lin, J. Synthesis of boron nitride nanotubes and its hydrogen uptake. *Catal. Today* **2007**, *120* (3-4), 346−350, DOI: 10.1016/j.cattod.2006.09.016.

(237) Lale, A.; Bernard, S.; Demirci, U. B. Boron nitride for hydrogen storage. *Chem.Plus.Chem.* **2018**, *83*, 893−903.

(238) Weng, Q.; Wang, X.; Zhi, C.; Bando, Y.; Golberg, D. Boron nitride porous microbelts for hydrogen storage. *ACS Nano* **2013**, *7*, 1558−1565.

(239) Salameh, C.; Moussa, G.; Bruma, A.; Fantozzi, G.; Malo, S.; Miele, P.; Demirci, U. B.; Bernard, S.; et al. Robust 3D boron nitride nanoscaffolds for remarkable hydrogen storage capacity from ammonia borane. *Energy Technol.* **2018**, *6*, 570−577.

(240) Nada, A. A.; Bekheet, M. F.; Viter, R.; Miele, P.; Roualdes, S.; Bechelany, M. BN/GdxTi(1-x)O(4-x)/2 nanofibers for enhanced photocatalytic hydrogen production under visible light. *Appl. Catal. B Environ.* **2019**, *251*, 76−86.

(241) Kawrani, S.; Nada, A.A.; Beckheet, M.F.; Boulos, M.; Viter, R.; Roualdes, S.; Miele, P.; Cornu, D.; Bechelany, M. Enhancement of calcium copper titanium oxide photoelectrochemical performance using boron nitride nanosheets. *Chem. Eng. J.* **2020**, *389*, No. 124326, DOI: 10.1016/j.cej.2020.124326.

(242) Mananghaya; Michael Rivera. Titanium-Decorated Boron Nitride Nanotube for Hydrogen Storage: A Multiscale Theoretical Investigation. *Nanoscale* **2019**, *11* (34), 16052−16062.

(243) Choyal, V.; Choyal, V.K.; Kundalwal, S.I. Effect of atom vacancies on eastic and electronic properties of transversely isotropic boron nitride nanotubes: A comprehensive computational study. *Comput. Mater. Sci.* **2019**, *156*, 332−345.

(244) Shahsavari, R.; Zhao, S. Merger of Energetic Affinity and Optimal Geometry Provides New Class of Boron Nitride Based Sorbents with Unprecedented Hydrogen Storage Capacity. *Small* **2018**, *14*, No. 1702863.

(245) Sakhavand, N.; Shahsavari, R. Synergistic Behavior of Tubes, Junctions, and Sheets Imparts Mechano-Mutable Functionality in 3D Porous Boron Nitride Nanostructures. *J. Phys. Chem. C* **2014**, *118* (39), 22730−22738.

(246) Colombo, P.; Mera, G.; Riedel, R.; Sorarù, G. D. Poly mer-Derived Ceramics: 40 Years of Research and Innovation in Advanced Ceramics. *J. Am. Ceram. Sci.* **2010**, *93* (7), 1805−1837, DOI: 10.1111/j.1551-2916.2010.03876.x.

(247) Idrees, M.; Batool, S.; Kong, J.; Zhuang, Q.; Liu, H.; Shao, Q.; Lu, N.; Feng, Y.; Wujcik, E. K.; Gao, Q.; Ding, T.; Wei, R.; Guo, Z. Polyborosilazane derived ceramics - Nitrogen sulfur dual doped graphene nanocomposite anode for enhanced lithium ion batteries. *Electrochim. Acta* **2019**, *296*, 925−937.

(248) Wan, J.; Mukherjee, A. K., M. J. Gasch. 7077991 US, 2006.

(249) Sarkar, S.; Zou, J.; Liu, J.; Xu, C.; An, L.; Zhai, L. Polymer-derived ceramic composite fibers with aligned pristine multiwalled carbon nanotubes. *ACS APplied Materials Interfaces* **2010**, *2*, 1150−1156.

(250) Bhandavat, R.; Singh, G. Stable and efficient Li-ion battery anodes prepared from polymer-derived silicon oxycarbide-carbon nanotube shell/core composites. *J. Phys. Chem.C* **2013**, *117*, 11899−11905.

(251) Graczyk-Zajac, M.; Fasel, C.; Riedel, R. Polymer-derived-SiCN ceramic/graphite composite as anode material with enhanced rate capability for lithium ion batteries. *J. Power Sources* **2011**, *196*, 6412−6418.

(252) David, L.; Bernard, S.; Gervais, C.; Miele, P.; Singh, G. Facile synthesis and high rate capability of silicon carbonitride/boron nitride composite with a sheet like Morphology. *J. Phys. Chem.C* **2015**, *119*, 2783−2791.

(253) Abass, M. A.; Syed, A. A.; Gervais, C.; Singh, G. Synthesis and electrochemical performance of a polymer-derived silicon oxycarbide/boron nitride nano tube composite. *RSC Adv.* **2017**, *35*, 21576−21584, DOI: 10.1039/C7RA01545C.

(254) Yu, S.; Wang, X.; Pang, H.; Zhang, R.; Song, W.; Fu, D.; Hayat, T.; Wang, X. Boron nitride-based materials for the removal of pollutants from aqueous solutions: a review. *Chem. Eng. J.* **2018**, *333*, 343−360.

(255) Lei, W.; Portehault, D.; Liu, D.; Qin, S.; Chen, Y. Porous boron nitride nanosheets For effective water cleaning. *Nat. Commun.* **2013**, *4*, 1777.

(256) Li, T.; Wang, L.; Zhang, K.; Xu, Y.; Long, X.; Gao, S.; Li, R.; Yao, Y. Freestanding boron nitride nanosheet films for ultrafast oil/water separation. *Small* **2016**, *12*, 4960−4965.

(257) Dong, G.; Li, H.; Chen, V. *Challenges and opportunities for mixed-matrix membranes for gas separation J. Mater. Chem.* **2013**, *1*, 4610−4630.

(258) Sanders, D. F.; Smith, Z. P.; Guo, R.; Robeson, L. M.; McGrath, J. E.; Paul, D. R.; Freeman, B. D. Energy-efficient polymeric gas separation membranes for a sustainable future: a review. *Polymer* **2013**, *54*, 4729−4761.

(259) Tul Muntha, S.; Kausar, A.; Siddiq, M. Progress in applications of polymer-based membranes in gas separation technology. *Polym.-Plast. Technol. Eng.* **2016**, *55* (12), 1282−1298, DOI: 10.1080/03602559.2016.1163592.

(260) Zhang, Y.; Shi, Q.; Liu, Y.; Wang, Y.; Meng, Z.; Xiao, C.; Deng, K.; Rao, D.; Lu, R. Hexagonal boron nitride with designed nanopores as a high-efficiency membrane for separating gaseous hydrogen from methane. *J. Phys. Chem. C* **2015**, *119*, 19826−19831.

(261) Wang, Y.; Low, Z.-X.; Zhang, H.; Chen, X.; Hou, J.; Seong, J. G.; Lee, Y. M.; Simon, G. P. Functionalized boron nitride nanosheets: a thermally rearranged polymer nanocomposite membrane for hydrogen separation. *Angew. Chem.* **2018**, *57* (49), 16056−16061, DOI: 10.1002/anie.201809126.

(262) Emanet, M.; Çulha, M.; Sen, O. Evaluation of boron nitride nanotubes and hexagonal boron nitrides as nanocarriers for cancer drugs. *Nanomed.* **2017**, *12* (7), 797−810, DOI: 10.2217/nnm-2016-0322.

(263) Cao, X.; Halder, A.; Tang, Y.; Hou, C.; Wang, H.; Duus, J. O.; Chi, Q. Engineering two-dimensional layered nanomaterials for wearable biomedical sensors and power devices. *Mater. Chem. Front.* **2018**, *2*, 1944−1986.

(264) Zhang, Y.; Wang, Y. N.; Sun, X. T.; Chen, L.; Xu, Z. R. Boron nitride nanosheet/CuS nanocomposites as mimetic peroxidase for

sensitive colorimetric detection of cholesterol. *Sensor. Actuator. B Chem.* **2017**, *246*, 118−126.

(265) Nagarajan, S.; Belaid, H.; Pochat-Bohatier, C.; Teyssier, C.; Iatsunskyi, I.; Coy, E.; Balme, S.; Cornu, D.; Miele, P.; Kalkura, N. S.; Cavailles, V.; Bechelany, M. Design of boron nitride/gelatin electrospun nanofibers for bone tissue engineering. *ACS Appl. Mater. Interfaces* **2017**, *9*, 33695−33706.

(266) Kim, K.B.; Jang, W.; Cho, J.Y.; Woo, S.B.; Jeon, D.H.; Ahn, J.H.; Hong, S.D.; Koo, H.Y.; Sung, T. H. Transparent and flexible piezoelectric sensor for detecting human movement with a boron nitride nanosheet (BNNS). *Nano Energy* **2018**, *54*, 91−98, DOI: 10.1016/j.nanoen.2018.09.056.

(267) Kang, J. H.; et al. Multifunctional electroactive nanocomposites based on piezoelectric boron nitride nanotubes. *ACS Nano* **2015**, *9* (12), 11942−11950.

(268) Thibeault, S. A., et al. Radiation shielding materials containing hydrogen boron, and nitrogen: systematic computational and experimental study phase I. *NIAC final report*; NASA: Langley, VA, 2012.

(269) Thibeault, S. A.; et al. Nanomaterials for radiation shielding. al. *MRS Bull.* **2015**, *40* (10), 836−841.

(270) Kim, J. H.; Pham, T. V.; Hwang, J. H.; Kim, C. S.; Kim, M. J. Boron nitride nanotubes: synthesis and applications. *Nano Convergence* **2018**, *5*, 17.

(271) Gao, Y.; Hong, Y.-L.; Wu, Z.; Yang, Z.; Chen, M.-L.; Liu, Z.; Ma, T.; Sun, D.-M.; Ni, Z.; Ma, X.-L.; Cheng, H.-M.; Ren, W. Ultrafast Growth of High-Quality Monolayer WSe2 on Au. *Adv. Mater.* **2005**, *29* (29), No. 1700990, DOI: 10.1002/adma.201700990.

(272) Bai, X. D.; Golberg, D.; Bando, Y.; Zhi, C. Y.; Tang, C. C.; Mitome, M.; Kurashima, K. Boron Nitride Nanotubes. *Nano Lett.* **2007**, *7*, 632.

(273) Fujii, M.; Zhang, X.; Xie, H.; Ago, H.; Takahashi, K.; Ikuta, T.; Abe, H.; Shimizu, T. Measuring the Thermal Conductivity of a Single Carbon. *Phys. Rev. Lett.* **2005**, *95*, No. 065502.

(274) Yao, Y.; Lin, Z.; Li, Z.; Song, X.; Moon, K. S.; Wong, C. P. *Large-scale production of two-dimensional nanosheets J. Mater. Chem.* **2012**, *22*, No. 13494.